Geochemistry International 41(4): 338-363, 2003

Petrogenesis of the Central Gabbroic Pluton in the Lake Zone, Western Mongolia

E. V. Borodina

Institute of Geology, Siberian Division, Russian Academy of Sciences,
pr. akademika Koptyuga 3, Novosibirsk, 630090 Russia
e-mail: borev@uiggm.nsc.ru

Abstract

The Central pluton in the Lake Zone, western Mongolia is a shallow-seated layered basic intrusion of the island-arc type. The pluton belongs to the Cambrian peridotite-pyroxenite-anorthosite-gabbronorite rock association, which is widespread in western Mongolia. It is composed of the chilled facies, marginal facies, and the layered series including ultramafic, subultramafic, mafic, and anorthosic rock groups. As follows from the character of layering, the pluton was formed in a single stage through the emplacement of an initial magma batch. The distribution of major and minor elements in cumulates and residual melt was modeled using the COMAGMAT 3.5 program. The results of calculations agree best with the real rock compositions at the following parameters: a pressure of 1 kbar, up to 0,5 wt % H_2O in the melt, and QFM buffer. The model primary melt contains 20 wt % MgO and 7 wt % FeO; 100*Mg/(Mg + Fe) = 83,59. It was established that the initial magma that filled the intrusive chamber already entrained about 20% of olivine crystals, which settled to the bottom of the chamber making up a basal peridodite unit. Olivine crystallized at a shallow depth in a transitional magma chamber. The rocks of the Central pluton and their parental melt are characterized by low REE contents similar to those of the primitive mantle and N-MORB source with Ta, Hf, Ti minimum and U and Th maximum; a marked depletion in HREE is typical. The relatively high U and Th contents, slight enrichment in LREE with (La/Yb)ch = 1,60-1,91, and Ta minimum in all rocks resemble the geochemical signature of the island-arc tholeiitic series. The distribution of HFSE and HREE, which are immobile during the dehydration of a subducted oceanic plate, characterizes the mantle matter similar to the N-MORB source, which existed before enrichment in mobile elements during subduction. The primary melt composition was modeled by the MELTS program. It corresponds to the melt that was formed through the batch partial melting of the depleted mantle source (garnet lherzolite) at a pressure of 25 kbar, a temperature of 1600C, 0,1 wt % H_2O in the source, and a degree of melting of ~20%. The Central pluton was emplaced in a primitive island-arc environment. However, it cannot be regarded as a direct hypabyssal comagmatic counterpart of the Cambrian high-alumina volcanics of the Lake Zone, because the latter have been contaminated by crustal materials and underwent magma mixing. The general geochemical similarity of volcanic and plutonic rocks supports the suggestion on the existence of a common subduction-related garnet-bearing mantle source.

Received in revised form July 3, 2001

INTRODUCTION

Peridotite-pyroxenite-anorthosite-gabbronorite plutons, which are regarded as shallow transitional magma chambers related to high-alumina island-arc basalts, are widespread in the Central Asian Foldbelt (CAFB) **[1]**. The Tuva-Mongolia Foldbelt **(Fig. 1)**, the longest within CAFB, comprises several intrusive clusters (Lake Hyargas, Bayantsagan, Dzabkhan, and Tugurik) **[2]**. The interest to these intrusions is roused by their bearing on the general problems of the evolution of island-arc volcanism, and, in particular, on the estimation of primary magma composition, its geochemical signature, composition of mantle magma sources, and magma fractionation in layered basic plutons. This work deals with the formation of layered gabbroid plutons exemplified by a layered intrusion of the Lake Hyargas Complex in western Mongolia. In particular, this work aimed at the estimation of parental magma composition and physicochemical conditions of its fractionation. The attention was focused on its geochemical features, the restoration of mantle source geochemistry, and principal stages of primary melt evolution from its generation to the formation of the layered series. The choice of the Central pluton as a subject of investigation was not accidental. In contrast to most plutons of the Lake Hyargas Complex, it has a simple internal structure, which resulted from one-stage filling of a magma chamber. Its marginal and chilled facies are clearly recognized. The complete set of rather fresh evolved rocks typical of layered plutons is well expressed. The newly obtained and published data **[1, 2]** on major and minor element contents were used. Rock-forming minerals were analyzed with a Camebax microprobe at the Analytical Center of the United Institute of Geology, Geophysics, and Mineralogy, Siberian Division, Russian Academy of Sciences, analyst L.N.Pospelova.

Fig. 1. Localization of peridotite-pyroxenite-gabbronorite plutons in eastern Tuva and northwestern Mongolia, after **[2]**.

(1) Precambrian basement; (2) volcanic dacite-andesite-basalt complexes and subordinate carbonate and terrigenous pelitic rocks; (3) carbonate and terrigenous rocks and subordinate volcanics; (4) Cambrian volcanics, cherts, shales and Cambrian and Ordovician flyschoid rocks; (5) Early Hercynian volcanosedimentary rocks; (6) Hercynian volcanosedimentary rocks; (7) Mesozoic and Cenozoic volcanosedimentary rocks; (8) faults; and (9) peridotite-pyroxenite-gabbronorite plutons.

Plutons of the Mazhalyk Complex in eastern Tuva (numerals in the map): 1 - Mazhalyk; 2 - Karashat; 3 - Kalbakdag; 4 - Brungan; 5 - Khang; 6 - Bashkhem; 7 - Elig-Khol; 8 - Khanchar; and 9 - Pogranichnyi. Plutons of the Lake Hyargas Complex in the Lake Zone, northwestern Mongolia: 10 - Zamyn; 11 - Central; 12 - Ulaan Ula; 13 - Harachulu; 14 - Tas Khairkhan; 15 - Sar Khairkhan; 16 - Dzabkhan; 17 - Bayantsagan; 18 - Khairhan; 19 - Tugurik; and 20 - Sukhontiin Har Ula. Plutons of the Tamir Complex in the Khangai mountain region of northwestern Mongolia: 21 - Ortsog Ula; 22 - Dulan Ula; 23 - Har Tologoi; 24 - Khargantuingol; 25 - Bayanbulak; 26 - Olonkhuduk; and 27 - Bumbeger.

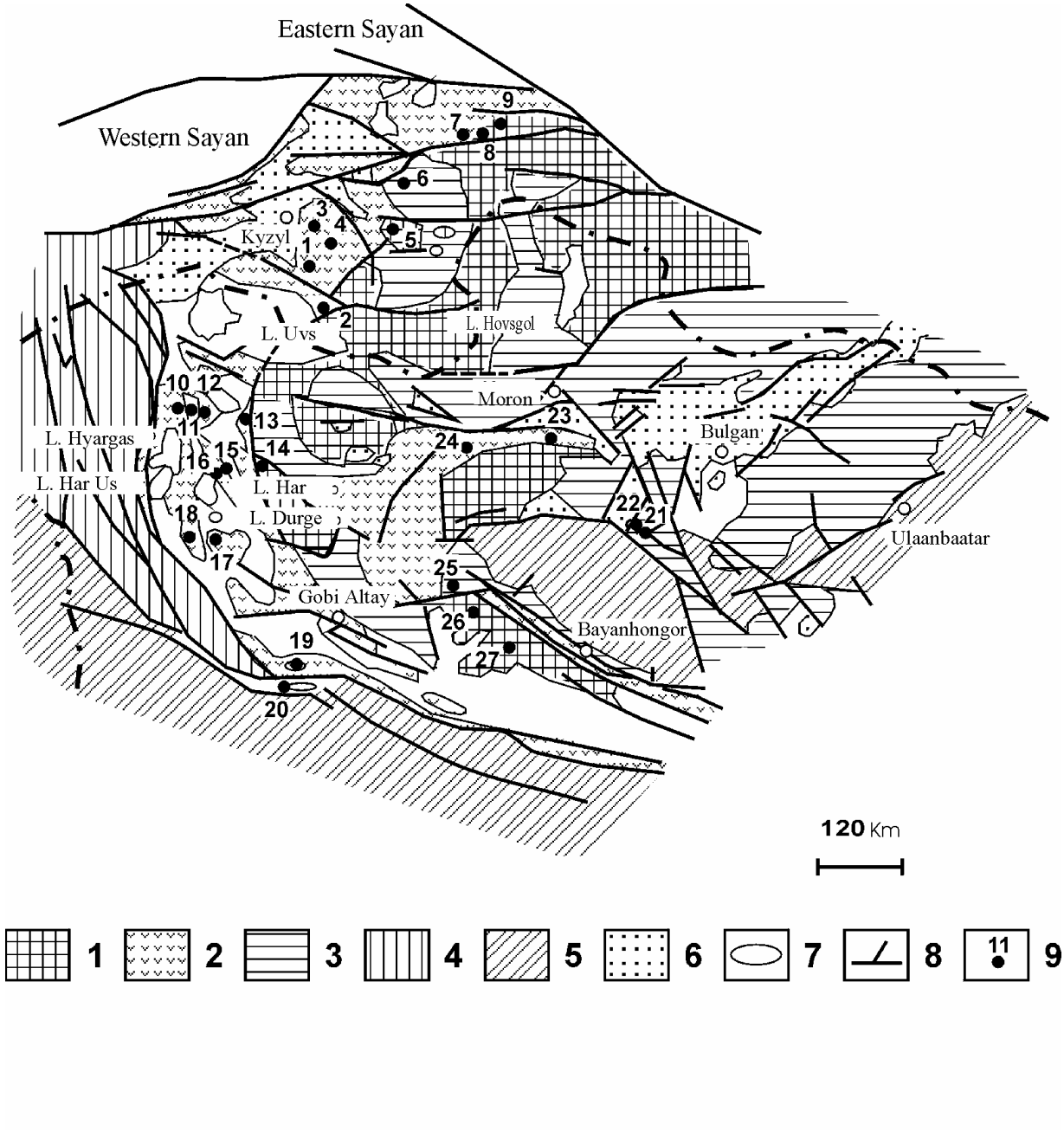

GEOLOGIC SETTING AND STRUCTURE OF THE PLUTON

The Central pluton **(Fig. 2)** is situated in the center of an intrusive cluster south of Lake Hyargas within the southern part of a diorite-granodiorite batholith belonging to the Tokhtogenshil Complex. The pluton is a small, oval-shaped in plan intrusion elongated in the latitudinal direction and divided into the Northern and Southern blocks by faults. The Northern block, 1.0 x 0.4 km in area, is largely composed of leucocratic rocks (olivine gabbro, olivine gabbronorite, leucograbbro, and anorthosite) making up the apical portion of the intrusion. The Southern block

is situated 2-3 km south of the Northern block, and its base is made up of a peridotitic cumulate unit, which grades upsection into more leucocratic rocks. Intrusive contacts with the country volcanosedimentary rocks are observed. Thin layers of skarn after limestone are cut off by the marginal facies of the intrusion. Gabbroic rocks contain xenoliths of porphyritic volcanics transformed into hornfels, and thin injections of amphibole gabbro penetrate the country rocks **[2]**. The concentrically zoned layering of the Central pluton with layers dipping toward the center at an angle of ~70^{o} and the negative relief forms point to the initial funnel-shaped morphology of the intrusive chamber. The pluton consists of the chilled zone, marginal zone, and layered series. Four rock groups are distinguished in the vertical section of the layered series by their mineralogy and cumulus assemblages (from bottom to top): (1) ultramafic (about 20% of the apparent thickness) with Ol + Sp cumulus assemblage, (2) subultramafic (20% of the section) with Ol + Pl and Ol + Pl + Cpx cumulus assemblages, (3) mafic (56% of the section) with Ol + Pl + Cpx + Opx and Pl + Cpx + Opx cumulus assemblages, and (4) anorthositic (4% of the section) with Pl cumulus assemblage **[2]**.

Fig. 2. Geological structure of the southern Central pluton, after **[2]**.
(1) Granitized basic volcanics; (2) shale with carbonate interlayers transformed into hornfels; (3) layered series; (4) basal unit of plagioclase peridotite; (5) marginal facies; (6) fine-grained granite and aplite; (7) diabase dikes; (8) faults; (9) strike and dip of layering and trachytoid structure in gabbroic rocks; and (10) quartz diorite and tonalite of the Tokhtogenshil Complex.

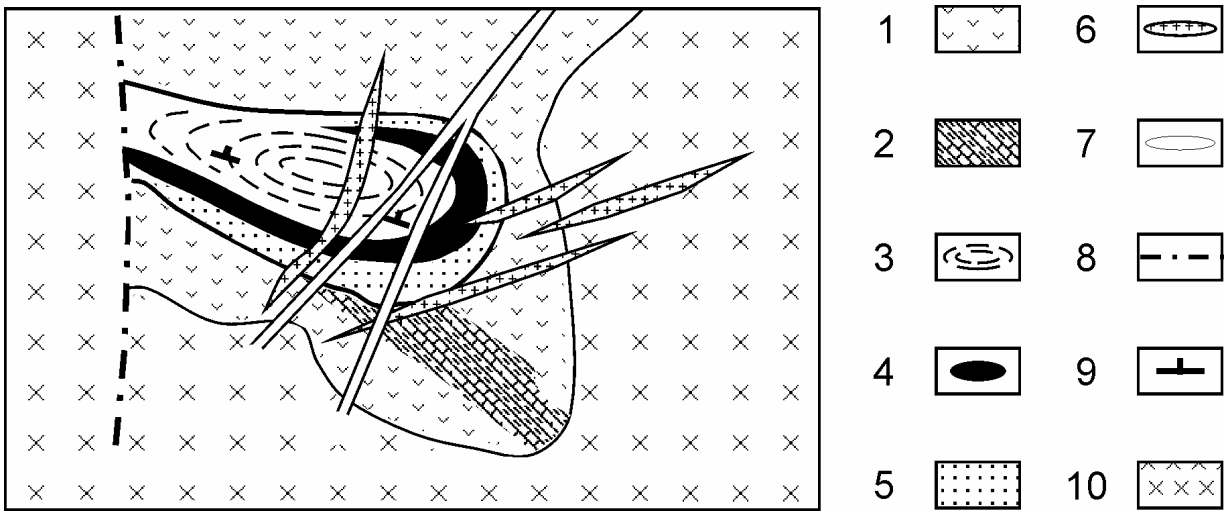

PETROGRAPHY OF THE CENTRAL PLUTON

The chilled and marginal facies of the Central pluton are composed of olivine gabbro and amphibole-olivine gabbro with abundant brown poikilitic amphibole. Owing to the small size of the intrusion and insignificant contact alteration, olivine is retained in the marginal zone. Therefore, the composition of the marginal facies (Sample I-2038) can be used for the estimation of parental magma composition **[2]**.

The rocks of the ultramafic group – plagioclase-bearing dunite and wehrlite – were formed as a result of early olivine settling **[3]**. The basal peridotite unit directly adjoins the rocks of the marginal facies and makes up a horseshoe-shaped body near the bottom of the intrusion unconformable to its internal structure **[4]**. The plagioclase-bearing dunite consists of olivine (85%), plagioclase (5%), clinopyroxene (5%), and orthopyroxene (5%). The wehrlite is composed of olivine (65-82%), plagioclase (1-4%), clinopyroxene (11-30%), and poikilitic brown amphibole (1-3%).

The subultramafic group comprises melanotroctolite (82% Ol, 14% Pl, and 4% Cpx) and melanocratic olivine gabbro (35-76% Ol, 8-14% Pl, and 14-45% Cpx).

The mafic group includes olivine gabbro (10-25% Ol, 25-45% Pl, 19-50% Cpx, and 0-5% Opx), amphibole gabbro (45-55% Pl, 10-13% Cpx, and 6-10% Amph), and leucogabbro (60% Pl, 35% Cpx, and 5% Opx).

The anorthositic group includes two types of anorthosite schlieren occurring both in the upper and lower parts of the section: (1) small conformable lenses and interlayers in the host gabbro and (2) irregular bodies discordant to the layering.

MINERALOGY OF ROCKS FROM THE CENTRAL PLUTON

Olivine is a rock-forming mineral of all rock groups except for the anorthositic group and part of the mafic group (this mineral is missing in the amphibole gabbro and leucogabbro). In the rocks of ultramafic and subultramafic groups, olivine is always euhedral relative to other minerals and is commonly partly serpentinized. Olivine, plagioclase, and clinopyroxene from the olivine gabbro may be equally euhedral, which indicates that all these minerals crystallized simultaneously. The olivine crystals attain 3 mm (occasionally, 4.5 mm) in diameter. Its magnesian number Mg# =100 Mg/(Mg + Fe) varies from 83.1 in the plagioclase peridotite and 84.1 in the troctolite to 82.1-75.5 in the olivine gabbro and 78.3-73.2 in the marginal facies of the pluton **(Fig. 3; Table 1)**. Euhedral Cr-spinel inclusions are typical of olivine from the basal peridotite unit (Sample I-1984a), whereas such inclusions were not observed in ultramafic units from the middle and upper parts of the layered series **[2]**. In all rocks, olivine shows no zoning or is only slightly zonal.

Fig. 3. Compositions of coexisting rock-forming minerals from the (1) layered series and (2) basal unit of the Central pluton in comparison with (3) mineral compositions obtained from modeling of layered intrusion formation. The primary magma crystallization was modeled at 1 kbar, QFM buffer, and 0.5 wt % H_2O in the melt.

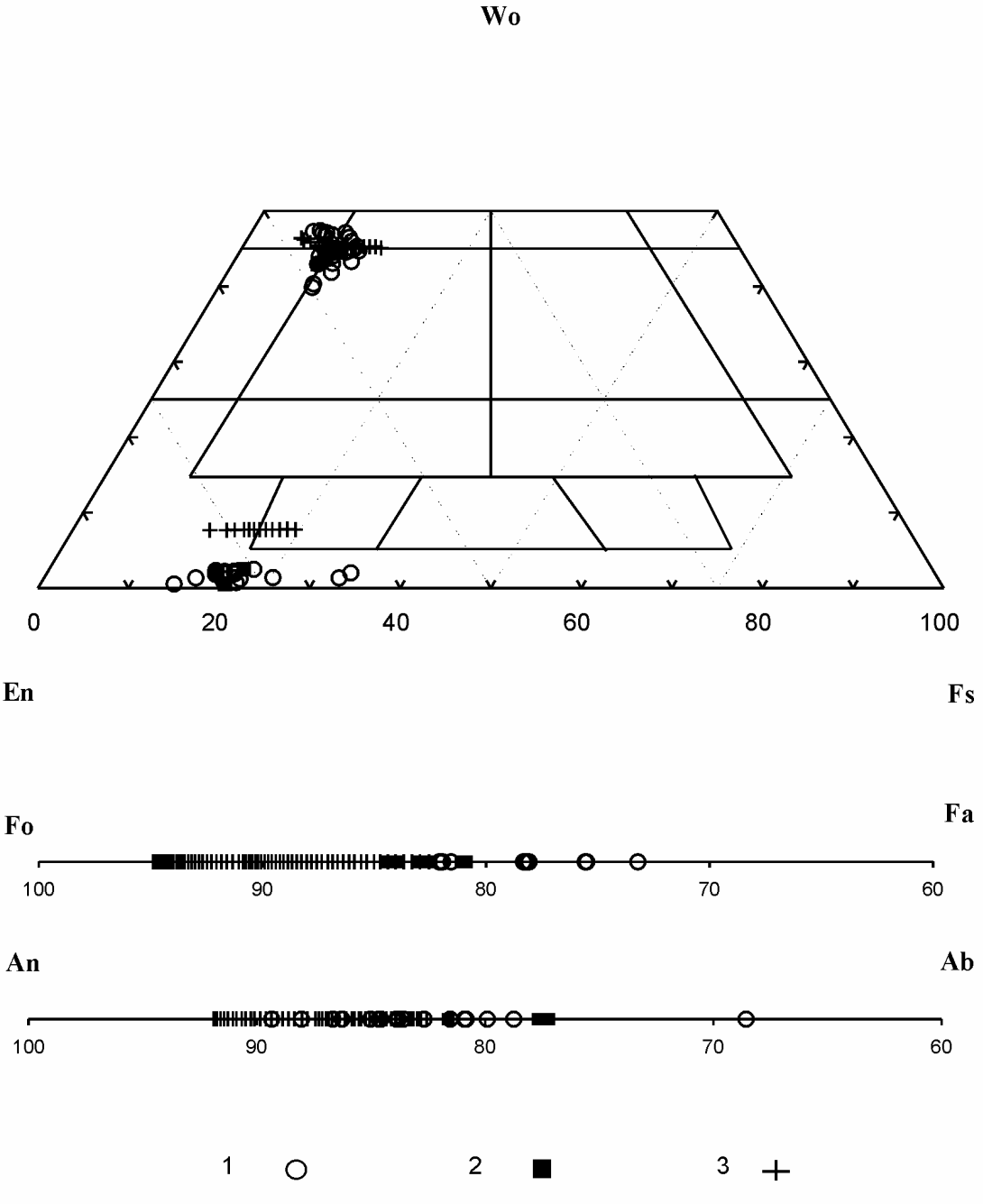
Wo
0
20
40
60
80
100
En
Fs
Fo
Fa
100
90
80
70
60
An
Ab
100
90
80
70
60
1
2
3

Table 1. The composition of olivine from the Central pluton, wt %

Component	Sample number						
	1 И-2036 Center	2 И-1983 Center	3 И-1984	4 И-1984	5 И-1984 Center	6 И-1984 Center	7 И-1984 Center
SiO_2	38,9	39,1	40,1	39,8	39,5	39,7	39,3
FeO	17,8	15,8	15,5	15,3	16,4	16,6	16,7
MgO	42,8	43,6	45,6	46,6	45,0	44,0	43,9
NiO	0,2	0,2	0,2	0,2	0,2	0,2	0,2
Total	99,7	98,7	101,5	101,9	101,1	100,5	100,0
Mg #	81,1	83,1	83,9	84,5	83,0	82,5	82,5
Ni(ppm)	1537	1512	0	166	1361	1415	1187
Cr(ppm)	89	180	61	428	0	0	246
FeO/MgO	0,42	0,36	0,34	0,33	0,37	0,38	0,38
Component	Sample number						
	8 И-1980 Center	9 И-1980 Center	10 И-1988 Center	11 И-2037 Margin	12 И-2037 Center	13 И-2030 Center	14 И-1981
SiO_2	37,7	37,8	39,5	39,2	39,0	38,9	38,8
FeO	18,8	18,9	17,0	22,4	22,4	19,8	20,1
MgO	44,5	44,7	43,6	38,6	38,8	39,8	40,2
NiO	0,1	0,1	0,1	0,1	0,1	0,1	0,1
Total	101,2	101,6	100,2	100,3	100,3	98,7	99,2
Mg #	80,9	80,9	82,1	75,5	75,6	78,2	78,2
Ni(ppm)	940	1075	1043	1136	674	1004	840
Cr(ppm)	216	108	89	20	109	0	62
FeO/MgO	0,42	0,42	0,39	0,58	0,58	0,50	0,50
Component	Sample number						
	15 И-2045 margin	16 И-2045 Center	17 И-2045 Center	18 И-2026 Center	19 И-2038 Margin	20 И-2038 Center	21 И-2038 Center
SiO_2	39,2	38,9	38,5	38,2	39,5	39,3	39,3
FeO	17,5	17,5	17,5	22,7	20,0	20,0	20,1
MgO	43,4	45,0	44,5	34,8	40,3	40,4	40,2
NiO	0,2	0,1	0,1	0,1	0,1	0,1	0,1
Total	100,2	101,5	100,6	95,9	100,0	99,8	99,7
Mg #	81,6	82,1	81,9	73,2	78,2	78,3	78,1
Ni(ppm)	1286	991	1164	664	762	842	788
Cr(ppm)	34	162	116	86	0	0	0
FeO/MgO	0,40	0,39	0,39	0,65	0,50	0,49	0,50

Note: 1 - Pl-bearing dunite, 2 - wehrlite, 3-7 - troctolite, 8, 9 - melanogabbro, 10-14 - olivine gabbro, 15-17 - amphibolized olivine gabbro, 18-21 - olivine gabbro of marginal facies. FeO is total iron. * After **[2]**.

Plagioclase from melanocratic rocks is anhedral with respect to olivine and together with clinopyroxene rims olivine grains and forms oikocrysts, up to 3 mm in size. In rocks of the mafic group, plagioclase is also anhedral relative to olivine; however, plagiocalse crystals are often tabular or irregular in shape and demonstrate the same degree of idiomorphism as clinopyroxene.

The size of plagioclase grains does not exceed 1-2 mm. The composition of analyzed homogeneous plagioclase crystals from the layered series varies from $An_{81.6}$ in the plagioclase peridotite to $An_{89.3-68.6}$ in the olivine gabbro and $An_{86.3-79.9}$ in the rocks of the marginal facies **(Fig. 3; Table 2)**. In general, intercumulus plagioclase from ultramafic rocks is less calcic ($An_{81.6}$) in comparison with plagioclase from olivine gabbro within the rhythms ($An_{89.3-68.2}$) **[2]**.

Table 2. The composition of plagioclase from the Central pluton, wt %

Component	Sample number									
	1 И-2036 Center	2 И-1984 Interstitial	3 И-1984 Interstitial	4 И-2037 Margin	5 И-2037 Center	6 И-1988	7 И-1981	8 И-1981	9 И-1989	10 И-2024 Center
SiO_2	47,7	46,5	47,3	46,3	48,5	47,3	46,2	46,5	45,8	50,8
TiO_2	0,1	0,0	0,1	0,1	0,1	0,1	0,0	0,1	0,0	0,0
Al_2O_3	33,2	32,7	32,4	34,3	33,1	33,3	34,1	33,7	33,4	30,8
FeO	0,3	0,2	0,3	0,4	0,4	0,2	0,3	0,4	0,3	0,4
CaO	16,7	15,7	15,3	17,2	16,7	16,9	17,9	17,4	17,4	14,5
Na_2O	2,1	2,5	2,5	1,5	1,8	2,0	1,2	1,3	1,7	3,6
K_2O	0,0	0,0	0,0	0,0	0,0	0,0	0,0	0,0	0,0	0,1
Total	100,1	97,8	97,9	99,6	100,5	99,7	99,7	99,3	98,7	100,2
An %	81,61	77,68	77,21	86,66	83,87	82,67	89,34	88,04	84,65	68,57
Ab %	18,29	22,24	22,68	13,32	16,04	17,31	10,58	11,84	15,17	31,04
Or %	0,09	0,08	0,11	0,02	0,08	0,02	0,08	0,12	0,19	0,38
Component	Sample number									
	11 И-2045	12 И-2045 Margin	13 И-2045 Center	14 И-2045 Center	15 И-2045 Margin	16 И-2026 Center	17 И-2026 Margin	18 И-2038 Margin	19 И-2038 Center	20 И-2038 Center
SiO_2	47,4	46,6	46,8	47,5	45,9	47,3	47,9	45,7	46,0	46,6
TiO_2	0,1	0,0	0,1	0,0	0,1	0,0	0,0	0,0	0,0	0,0
Al_2O_3	33,1	32,7	33,0	32,5	33,3	33,6	32,6	33,5	33,5	33,0
FeO	0,4	0,3	0,4	0,4	0,4	0,4	0,3	0,3	0,3	0,4
CaO	16,4	16,4	16,5	16,3	17,3	16,9	16,5	17,8	17,5	16,9
Na_2O	2,0	2,4	2,2	2,1	1,7	1,8	2,3	1,6	1,8	1,8
K_2O	0,0	0,0	0,0	0,0	0,0	0,0	0,0	0,0	0,0	0,0
Total	99,3	98,6	99,0	98,9	98,7	100,1	99,7	98,8	99,0	98,8
An %	81,52	78,74	80,83	80,91	85,02	83,79	79,90	86,27	84,57	83,59
Ab %	18,41	21,11	19,03	18,86	14,83	16,02	19,83	13,61	15,33	16,23
Or %	0,07	0,15	0,14	0,22	0,16	0,19	0,27	0,12	0,10	0,18

Note: 1 - Pl-bearing dunite, 2, 3 - troctolite, 4-9 - olivine gabbro, 10-15 - amphibolized olivine gabbro, 16-20 - olivine gabbro of marginal facies. FeO is total iron.

Clinopyroxene occurs in varying amount in all rock groups of the Central pluton. Clinopyroxene from the plagioclase peridotite is anhedral and fills the interstitial space between olivine crystals, rims these crystals, or occurs as oikocrysts, up to 1-3 mm in size. The clinopyroxene-plagioclase relationships in the wehrlite and olivine gabbro point to the joint crystallization of both minerals. Clinopyroxene from the layered series of the Central pluton corresponds to the diopside-salite-augite series ($En_{49.8-42.2}Fs_{13.1--6.8}Wo_{47.4--39.9}$); its Mg# varies

from 86.8-80.0 in the plagioclase peridotite and melanogabbro to 87.5-78.5 in the olivine gabbro and 85.0-77.9 in the rocks of the marginal facies **(Fig. 3; Table 3)**.

Table 3. The composition of clinopyroxene from the Central pluton, wt %

Component	Sample number										
	1	2	3	4	5	6	7	8	9	10	11
	И-2036 Center	И-1983 Center	И-1984 Interstitial	8433*	8433*	И-1980 Center	И-2028	И1989*	И-1989	И-1981	И-1981
SiO_2	50,1	50,8	50,4	51,6	50,6	50,0	54,0	51,9	51,3	51,3	52,4
TiO_2	0,9	0,7	0,6	0,5	0,3	0,2	0,1	0,2	0,4	0,2	0,3
Al_2O_3	4,4	3,9	4,0	2,7	4,3	2,4	1,0	3,7	3,6	3,4	3,0
FeO	5,6	5,2	5,1	6,8	6,1	4,6	4,5	5,5	5,0	4,8	5,2
MnO				0,2	0,2			0,2			
MgO	15,1	16,0	16,6	15,3	15,2	17,0	15,9	15,8	15,6	16,3	15,7
CaO	21,6	21,2	20,9	21,8	22,2	23,6	23,2	22,0	22,9	20,8	22,4
Na_2O	0,4	0,4	0,3	0,3	0,2	0,3	0,2	0,2	0,5	0,3	0,2
K_2O	0,0	0,0	0,0	0,0	0,0	0,0	0,0	0,0	0,0	0,0	0,0
NiO	0,1	0,0	0,0			0,0	0,0		0,0	0,0	0,0
Cr_2O_3	0,9	0,8	0,9	0,1	0,5	0,7	0,3	0,4	0,4	0,8	0,5
Total	99,0	98,9	98,7	99,2	99,6	98,7	99,2	99,7	99,7	98,0	99,6
Mg #	82,9	84,5	85,3	80,0	81,5	86,8	86,4	83,8	84,8	85,9	84,4
Ni(ppm)	429	286	350			342	119		134	273	47
Cr(ppm)	6204	5449	5891	479	3694	4706	1862	2531	2894	5488	3735
En %	44,36	46,32	47,56	43,40	43,74	45,97	45,10	45,38	44,10	47,66	45,18
Fs %	10,64	9,86	9,47	11,90	11,72	6,79	7,92	10,58	9,07	9,40	9,70
Wo %	45,00	43,82	42,98	44,70	44,54	47,24	46,98	44,03	46,83	42,94	45,12
FeO/MgO	0,37	0,33	0,31	0,40	0,40	0,27	0,28	0,34	0,32	0,29	0,33
Component	Sample number										
	12	13	14	15	16	17	18	19	20	21	22
	И2027*	П5729*	И2037*	И-2037 Center	И-2037 Margin	И-2024 Center	И2035*	И2035*	И2045*	И-2045 Margin	И-2045 Center
SiO_2	52,1	52,0	52,3	52,5	51,7	52,9	52,4	53,4	51,5	51,6	51,1
TiO_2	0,3	0,3	0,6	0,3	0,5	0,4	0,5	0,3	0,5	0,5	0,5
Al_2O_3	3,6	3,1	2,5	2,6	3,3	2,1	2,3	2,3	3,6	3,9	3,8
FeO	6,4	4,3	7,1	6,1	5,8	7,4	4,8	4,2	5,9	4,9	5,3
MnO	0,2	0,4	0,2				0,2	0,1	0,2		
MgO	16,6	16,0	14,8	15,5	15,8	15,2	16,0	16,3	14,7	16,6	16,2
CaO	21,2	23,3	21,9	22,0	21,9	20,8	23,6	24,1	22,9	21,7	21,7
Na_2O	0,1	0,2	0,4	0,3	0,3	0,5	0,2	0,1	0,2	0,4	0,4
K_2O		0,0		0,0	0,0	0,0	0,0	0,0	0,0	0,0	0,0
NiO				0,0	0,0	0,0				0,0	0,0
Cr_2O_3	0,3	0,8	0,2	0,1	0,1	0,2	0,3	0,2	0,1	0,9	0,8
Total	100,7	100,3	100,1	99,4	99,3	99,4	100,2	101,0	99,7	100,4	99,8
Mg #	82,3	87,0	78,8	81,9	83,0	78,5	85,6	87,5	81,5	85,9	84,6
Ni(ppm)				198	253	8				180	252
Cr(ppm)	1710	5131	1368	874	827	1300	2326	1300	753	5835	5593
En %	46,67	44,97	42,15	44,19	45,04	43,76	44,56	45,14	42,38	46,92	46,08
Fs %	11,48	8,40	12,58	10,86	10,44	12,96	8,35	7,48	11,15	9,08	9,63
Wo %	41,85	46,63	45,27	44,95	44,52	43,28	47,10	47,39	46,47	44,00	44,29
FeO/MgO	0,38	0,27	0,48	0,39	0,37	0,49	0,30	0,26	0,40	0,29	0,33
Component	Sample number										
	23	24	25	26	27	28	29	30	31	32	33

	И-2045 Center	И-2026 Margin	И-2026 Center	И-2026 Margin	И-2026 Center	И2026*	И-2038 Margin	И-2038 Center	И-2038 Center	И-2038 Margin	И-2038 Center
SiO_2	50,3	51,8	52,7	53,3	53,7	51,7	52,9	53,4	51,9	50,8	50,6
TiO_2	0,5	0,5	0,1	0,2	0,1	0,3	0,2	0,1	0,2	0,3	0,4
Al_2O_3	4,2	2,7	1,9	1,9	1,1	3,7	2,0	1,6	2,5	2,7	3,4
FeO	5,5	7,3	6,9	6,8	6,2	5,6	5,8	5,7	5,2	5,1	6,1
MnO						0,2					
MgO	17,3	14,5	14,7	15,0	15,1	15,8	15,8	16,0	15,5	16,2	17,7
CaO	19,3	21,3	21,4	22,6	23,4	21,2	21,9	22,1	22,1	22,2	19,8
Na_2O	0,3	0,5	0,4	0,3	0,2	0,2	0,4	0,3	0,3	0,3	0,3
K_2O	0,0	0,0	0,0	0,0	0,0	0,0	0,0	0,0	0,0	0,0	0,0
NiO	0,0	0,0	0,0	0,0	0,0		0,0	0,0	0,0	0,0	0,0
Cr_2O_3	0,7	0,1	0,1	0,1	0,1	0,4	0,2	0,2	0,5	0,5	0,5
Total	98,2	98,7	98,2	100,3	99,8	99,0	99,2	99,2	98,4	98,1	98,7
Mg #	84,8	77,9	79,1	79,8	81,3	83,5	82,8	83,3	84,2	84,9	83,8
Ni(ppm)	248	103	240	219	87		150	16	287	16	215
Cr(ppm)	4814	859	571	553	487	2873	1413	1317	3608	3725	3298
En %	49,78	42,22	42,72	42,42	42,49	45,93	44,76	45,20	44,80	45,93	49,42
Fs %	10,37	13,08	12,39	11,64	10,41	11,01	10,24	9,92	9,58	8,79	10,27
Wo %	39,85	44,69	44,89	45,94	47,11	43,06	45,00	44,87	45,63	45,28	40,31
FeO/MgO	0,32	0,51	0,47	0,45	0,41	0,35	0,37	0,36	0,33	0,32	0,34

Note: 1 - Pl-bearing dunite, 2 - wehrlite, 3 - troctolite, 4-7 - melanogabbro, 8-16 - olivine gabbro, 17-23 - amphibolized olivine gabbro, 24-33 - olivine gabbro of marginal facies. FeO is total iron. * After **[2]**.

Orthopyroxene is not abundant in the Central pluton. The mineral occurs as tabular crystals and sporadically as irregular grains anhedral relative to olivine and as oikocrysts, up to 1 mm in size. Orthopyroxene corresponds to hypersthene-bronzite ($En_{79.5\text{-}64.4}Fs_{33.6\text{-}18.5}Wo_{2.5\text{-}0.6}$) in composition; its Mg# varies from 81.5-78.7 in the plagioclase peridotite and troctolite to 81.9-66.6 in the olivine gabbro and 79.5-67.6 in the rocks of the marginal facies **(Fig. 3. Table 4)**.

Table 4. The composition of orthopyroxene from the Central pluton, wt %

Component	Sample number										
	1 И1962*	2 И1984*	3 И1984*	4 И1989*	5 И-2030 Center	6 И2027*	7 И-1981 oikocryst	8 И-1989 Center	9 И-1988	10 И-1988 Center	11 И-1989
SiO_2	54,7	56,0	54,9	53,7	54,9	54,8	54,5	57,5	54,9	54,8	52,3
TiO_2	0,3	0,1	0,1	0,2	0,1	0,1	0,2	0,2	0,2	0,1	0,0
Al_2O_3	1,5	1,4	2,5	0,7	1,4	1,8	2,2	1,9	2,3	1,9	1,7
FeO	13,6	12,2	12,6	20,8	12,5	12,3	13,2	10,9	11,6	11,5	11,9
MnO	0,3	0,3	0,2	0,7		0,3					
MgO	28,3	30,3	29,3	23,2	29,2	29,3	28,7	26,3	29,3	28,9	34,7
CaO	1,2	1,1	0,2	0,9	1,0	1,1	1,1	0,9	1,1	0,9	0,2
Na_2O	0,0	0,0	0,0	0,0	0,0	0,0	0,0	0,0	0,0	0,0	0,0
NiO					0,0		0,0	0,0	0,1	0,0	0,0
Cr_2O_3	0,0	0,0	0,0	0,0	0,0	0,0	0,1	0,4	0,4	0,1	0,0
Total	100,0	101,5	99,8	100,2	99,2	99,8	100,1	98,1	99,8	98,3	100,9
Mg #	78,7	81,5	80,6	66,6	80,6	80,9	79,5	81,1	81,9	81,8	83,9
Ni(ppm)					220		259	189	440	291	

Cr(ppm)	205	137	274	205	338	274	1004	3019	2412	884	
En %	76,02	79,23	79,04	64,43	78,57	78,28	77,19	77,32	79,19	79,48	84,68
Fs %	21,46	18,71	20,37	33,55	19,36	19,50	20,56	20,77	18,49	18,70	14,76
Wo %	2,51	2,06	0,60	2,02	2,07	2,22	2,25	1,91	2,32	1,82	0,56
FeO/MgO	0,48	0,40	0,43	0,89	0,43	0,42	0,46	0,42	0,39	0,40	

Component	Sample number						
	12 И-1989	13 И-2026	14 И2026*	15 И1964*	16 И1964*	17 И2038*	18 И2038*
SiO_2	53,8	54,5	53,5	55,0	55,7	54,8	53,8
TiO_2	0,0	0,1	0,2	0,1	0,1	0,3	0,1
Al_2O_3	1,3	1,4	0,8	1,1	1,8	1,6	3,8
FeO	11,7	14,8	20,3	15,8	13,9	13,2	13,7
MnO			0,5	0,6	0,3	0,3	0,3
MgO	31,5	28,0	23,8	27,1	29,6	28,8	29,2
CaO	0,7	1,2	0,6	0,7	0,4	1,0	0,6
Na_2O	0,0	0,0	0,0	0,0	0,0	0,0	0,1
NiO	0,0	0,0					
Cr_2O_3	0,1	0,0	0,0	0,0	0,0	0,1	0,0
Total	99,1	100,1	99,6	100,4	101,8	100,3	101,6
Mg #	82,8	77,1	67,6	75,4	79,1	79,5	79,2
Ni(ppm)	165	361					
Cr(ppm)		321	205	137	137	889	68
En %	81,90	74,92	66,08	73,36	77,76	77,16	77,07
Fs %	16,74	22,58	32,56	25,22	21,52	20,75	21,71
Wo %	1,36	2,50	1,36	1,41	0,72	2,09	1,22
FeO/MgO	0,37	0,53	0,85	0,58	0,47	0,46	0,47

Note: 1 - plagioclase peridotite, 2, 3 - troctolite, 4-12 - olivine gabbro, 13-18 - olivine gabbro of marginal facies. FeO is total iron. * After **[2]**.

Amphibole from the Central pluton is subdivided into two types. Primary late magmatic brown amphibole forms irregular anhedral grains, rims around other minerals, and large (3-6 mm) oikocrysts. Its content does not exceed 3-10 vol %. Secondary green amphibole, which replaces clino- and orthopyroxene, commonly accounts for no more than 3-5% of the rock volume but its amount increases up to 20-35 vol % in the zones of intense amphibolization, where large (up to 5 mm) oikocrysts are typical. The composition of the magmatic amphibole is presented in **Table 5**. The Mg# varies from 79.3 in the wehrlite (Sample I-1983) to 70.1 in the olivine gabbro of the marginal facies (Sample I-2026).

Table 5. The composition of amphibole from the Central pluton, wt %

Component	Sample number						
	1 И-1983	2 И-2030 Center	3 И-1981	4 И-1981	5 И-2045 Margin	6 И-2045	7 И-2026 Margin
SiO2	44,7	43,6	43,1	43,6	43,1	44,0	43,4
TiO2	0,1	2,3	2,7	2,4	3,2	1,7	1,2
Al2O3	12,7	11,6	11,5	11,6	12,1	12,0	11,7
FeO	8,3	9,6	9,0	8,9	8,0	8,7	11,3

MgO	17,8	15,4	15,9	16,0	16,4	17,7	14,8
CaO	10,5	11,6	11,3	11,1	11,7	11,2	11,1
Na2O	2,4	2,3	2,2	1,9	2,3	2,1	2,4
K2O	0,1	0,8	0,4	0,4	0,3	0,4	0,8
Cr2O3	0,0	0,2	0,1	0,1	0,5	0,4	0,1
Total	96,6	97,6	96,1	96,1	97,6	98,2	96,8
Mg #	79,3	74,1	75,9	76,2	78,4	78,4	70,1
Ni(ppm)	269	346	270	360	346	368	138
Cr(ppm)	0	1536	954	520	3780	3010	926
FeO/MgO	0,47	0,62	0,57	0,56	0,49	0,49	0,76

Note: 1 - wehrlite, 2-4 - olivine gabbro, 5, 6 - amphibolized olivine gabbro, 7 - olivine gabbro of marginal facies. FeO is total iron.

Magnetite is the most abundant oxide mineral. Magnetite amounts at 1-2% and, occasionally, up to 4-5% and occurs in all rocks of the layered series. Magnetite is commonly observed as dispersed dusty aggregates and irregular segregations; aggregates and schlieren, up to 5 mm in size, are noticed in melanocratic rocks. Magnetite is a secondary mineral in the Central pluton and was formed as a by-product of olivine serpentinization under an elevated oxygen partial pressure **[5]**. The notable amount of secondary magnetite in the rocks of the Central pluton clearly indicates rather high Fe/(Fe + Mg) ratio of olivine.

The composition of olivine from the Central pluton varies from $Fo_{84.5}$ to $Fo_{73.2}$, and that of plagioclase ranges from $An_{89.3}$ to $An_{68.6}$ **(Fig. 3)**. The following cumulus mineral assemblages are observed:

1. Sample I-1984 (troctolite): $Fo_{83.9}$ + $An_{77.7}$ + Cpx (Mg# =85.3) + Opx (Mg# =80.6);
2. Sample I-1981 (olivine gabbro): $Fo_{78.2}$ + $An_{89.3}$ + Cpx (Mg# =85.9) + Opx (Mg# =79.5);
3. Sample I-2026 (olivine gabbro of the marginal facies): $Fo_{73.2}$ + $An_{83.8}$ + Cpx (Mg# =83.5) + Opx (Mg# =77.1);
4. Sample I-2038 (olivine gabbro of the marginal facies): $Fo_{78.3}$ + $An_{86.3}$ + Cpx (Mg# 85.0) + Opx (Mg# =79.5).

RESULTS OF COMPUTER MODELING

The COMAGMAT 3.5 program **[6]** was used in this work. The program allows modeling of the fractional crystallization and formation of the layered intrusion issuing from the given melt composition. The aim of modeling was to estimate the fractionation conditions that provide the evolution trends of major and trace elements corresponding to the observed geochemical characteristics of the layered pluton **[7]**. The bulk composition of the marginal facies of the Central pluton (Sample I-2038), which was regarded as a parental melt composition, and the calculated composition of primary melt **(Table 6)** were chosen as starting compositions in computation. The parental melt filled the intrusive chamber, and the primary melt was produced in the mantle source. The primary magma composition was calculated from the assumption that the intruding magma already contained olivine crystals, which precipitated from the primary melt at shallow depths, and the liquid fraction corresponded to the parental melt. This assumption is

based on the results of modeling by the COMAGMAT 3.5 program **(Fig. 4)**. The computation was performed in the regime of layered pluton formation under the following parameters: a pressure of 1 kbar, QFM buffer, and 0-5 wt % H_2O in the melt. The computation has shown that the peridotite cumulate should account for 5-7 vol % of the layered series under these conditions. At the same time, the ultramafic unit occupies in fact more than 20 vol % of the section. The magma probably contained 15-20 vol % of excess olivine at the moment of emplacement into the chamber. The primary magma composition was calculated using the olivine/melt partition coefficients **[13]** and was subsequently corrected by the COMAGMAT 3.5 program so that the volume of monomineral olivine cumulates would be no less than 20% and fractional crystallization at a shallow depth would result in the formation of melt close in composition to the parental liquid. Trace element contents, except for REE, were estimated approximately by fitting. However, the Ni content of the primary melt (440 ppm) can be calculated directly from the assumption that olivine from the ultramafic cumulate unit (Sample I-2036) with the maximum Ni content of 1537 ppm was a liquidus phase. The Ni content of the primary melt (Ni_{liq}) equals Ni_{ol}/D_{Ni}(ol/liq), where Ni_{ol} is the Ni content of the liquidus olivine, D_{Ni}(ol/liq) is the partition coefficient of Ni between olivine and melt determined from the formula D_{Ni}(ol/liq) = 3.92*D_{MgO}(ol/liq)-5.3 **[14]**. The D_{MgO}(ol/liq) value can be calculated as a ratio of the MgO content of the liquidus olivine (42.8 wt %) to the MgO content of the primary melt (20 wt %) **(Table 1)**. It follows that the Ni content of the primary melt was no less than 440 ppm. The choice of computation parameters for the layered pluton modeling was based on the mineralogy of the Central pluton. For example, the presence of cumulus orthopyroxene at the late stage of crystalliztaion constrains the water content of the melt as <0.5 wt % and the total pressure as <2 kbar. The emplacement of magma at low pressure is also consistent with the development of a hornfels aureole around the pluton. The Cr-spinel inclusions in olivine crystals from the peridotite unit suggest that oxygen fugacity (fO_2) was above the NNO buffer at the initial stage of parental magma crystallization **[15]**. The value of fO_2 was most probably within the QFM-NNO range. The comparison of the model and real mineral compositions from the rocks of the Central pluton testifies that the model parameters adequately reproduced the natural conditions **(Tables 1-5)**. The formation of the layered pluton was modeled with a crystallization step of 1 mol % at a pressure of 1 kbar, QFM buffer, and 0.5 wt % H_2O in the melt. The range of model plagioclase compositions ($An_{92.6-79.0}$) almost completely overlaps the range of natural plagioclase composition from the layered series ($An_{89.3-77.2}$). The calculated olivine compositions ($Fo_{94.7-76.6}$) are slightly enriched in Fo relative to the compositions of natural olivine ($Fo_{84.5-73.2}$), which is suggested to be more altered than the coexisting plagioclase. Model clinopyroxene compositions ($En_{48.2-40.9}Fs_{13-4}Wo_{47.9-46.0}$) coincide with natural compositions ($En_{49.8-42.2}Fs_{13.1-6.8}Wo_{47.4-39.9}$) and fall on the boundary of the diopside-salite-augite fields **(Fig. 3)**. Orthopyroxene from the Central pluton corresponds to hypersthene-bronzite in composition ($En_{84.7-64.4}Fs_{33.6-14.8}Wo_{2.5-0.6}$). The model orthopyroxene ($En_{72.9-70.0}Fs_{20.1-19.2}Wo_{7.67-7.90}$) is enriched in Wo, but is generally similar to the natural mineral. Olivine from the basal unit ($Fo_{84.5-80.9}$) is enriched in Fo relative to olivine from the layered series ($Fo_{82.1-73.2}$). In contrast, plagioclase from the mafic rocks ($An_{81.6-77.2}$) contains less An than that from the layered series ($An_{89.3-78.7}$). This implies that the plagioclase of peridotite crystallized from low-Mg residual melt and filled the interstitial space between olivine crystals, while plagioclase was a liquidus mineral in the layered series and crystallized from high-Mg melt together with olivine or somewhat later. The calculated trends of major and minor elements versus MgO content, which is used as a differentiation index, **(Fig. 5)** are generally consistent with the sequential crystallization of cumulus minerals (olivine, plagioclase, and

clinopyroxene) from the primary melt. The transition from the high-Mg to low-Mg rocks is accompanied by a systematic increase in Si, Ti, Al, Fe, Ca, Na, K, Cu, and La contents and monotonous depletion in Ni. In general, the model trends of cumulus phases coincide with the observed cumulate sequence of the layered series of the Central pluton **(Fig. 5)**, which suggests that the selected model parameters and compositions were similar to the characteristics of real primary melts. The compositions of model residual melts are shown in Fig. 6. The trends of evolved melt compositions computed with the COMAGMAT 3.5 program at 1 kbar pressure, 0.5 wt % H_2O in the melt, QFM buffer, and at the highest degree of crystallization of 80% were compared with the estimates obtained by the MELTS **[12]** program at the same conditions. A notable difference in evolved melt compositions was recorded only when the degree of crystallization exceeded 40-50%. At lower degrees of crystallization, the computation results from both programs were in good agreement. The Vendian and Cambrian volcanics of the Lake Zone **[16]** and coeval basalts of the Irbitei sequence in the eastern Tannu-Ola **[1]** form a separate compositional field **(Fig. 6)**, which lies out of the general trend of the Central pluton for all components except Al and Ti. Modeling with the COMAGMAT 3.5 program failed to reproduce the composition of the volcanic rocks from the primary melt of the Central pluton even by changing fractionation parameters and assuming a multistage process. This implies that the Central pluton cannot be regarded as a direct comagmatic counterpart of the coeval high-Al volcanics of the Lake Zone without involvement of other processes, such as magma mixing and crustal contamination.

Table 6. The composition of rocks and model melts (major elements are in wt %, trace elements, in ppm)

Component	1	2	3	4	5	6	7	8	9	10	11	12	13
SiO_2	47,37	47,45	46,83	47,88	45,50		50,73	45,32		47,34	47,67	43,05	42,11
TiO_2	0,33	0,36	0,32	0,38	0,25		1,37	0,22	0,19	0,21	0,10	0,39	0,65
Al_2O_3	15,65	15,39	13,50	16,20	14,36		15,30	4,67		4,05	3,90	11,50	11,63
FeO	6,52	6,44	7,00	7,18	8,64		9,37	7,92		5,40	6,00	8,51	11,15
MnO		0,10	0,10	0,11			0,18	0,13		0,10	0,10	0,54	0,45
MgO	13,35	13,66	20,00	13,55	18,88		9,02	37,55		39,14	39,00	21,78	21,12
CaO	15,75	15,63	11,20	13,44	11,35		11,48	3,76		3,11	3,00	12,48	11,48
Na_2O	0,90	0,88	0,90	1,08	0,88		2,32	0,37		0,52	0,20	0,99	1,25
K_2O	0,08	0,07	0,09	0,11	0,08		0,09	0,03	0,01	0,10	0,02	0,11	0,10
P_2O_5	0,05	0,03	0,06	0,07	0,04		0,14	0,02		0,03	0,01	0,05	0,07
H_2O			0,50	0,59							0,10	0,54	0,35
Mg #	78,50	79,09	83,59	77,09	79,58		63,18	89,42		92,82	92,06	82,02	77,15
La		1,50	1,25	1,50		0,31	2,50	0,69	0,29				
Ce		3,70	3,10	3,72		0,81	7,50	1,78	0,96				
Nd		2,40	2,00	2,40		0,60	7,30	1,35	0,93				
Sm		0,70	0,58	0,70		0,20	2,63	0,44	0,35				
Eu		0,30	0,25	0,30		0,07	1,02	0,17	0,14				
Gd		0,90	0,75	0,90		0,26	3,68	0,60	0,50				
Tb		0,20				0,05	0,67	0,11	0,09				
Yb		0,53	0,44	0,53		0,21	3,05	0,49	0,42				
Lu		0,08	0,07	0,08		0,03	0,46	0,07	0,06				
Hf		0,24					2,05	0,31	0,23				
Ta		0,02					0,13	0,04					
Y							28,00	4,55	4,06				
Nb							2,33	0,71	0,19				

Zr							74,00	11,20	8,14				
Th		0,20					0,12	0,09	0,01				
U		0,30	0,24				0,05	0,02	0,00				
Cs							0,01	0,03	0,00				
Rb							0,56	0,64	0,06				
Ba							6,30	6,99	0,61				
Cu		100	90	107				30					
Ni		185	440	159			177	1890		2358	2362		
Co		44	50	50			50	110					
Cr		730	750	764			346	2940		2736			
CIPW, вес%													
Or	0,47	0,41	0,53	0,64	0,47								
Ab	7,59	7,45	7,62	9,14	7,48								
An	38,32	37,84	32,54	39,04	35,00								
Di	31,49	31,66	18,03	21,83	16,87								
Hy	0,00	0,50	7,41	9,00	1,87								
Ol	21,39	21,40	33,13	19,46	37,74								
Ilm	0,62	0,68	0,61	0,72	0,48								
Ap	0,12	0,07	0,14	0,17	0,09								

Note: (1) Average composition of the marginal facies of the Central pluton **[2]**; (2) composition of the marginal facies, Sample I-2038 **[2]** corresponding to the parental magma composition by the moment of emplacement; (3) calculated bulk composition of the primary magma. According to the accepted model, the primary magma contained 20% of olivine crystals at the onset of emplacement, while the liquid phase corresponded to the parental magma in composition. (4) Model residual melt (melt composition after crystallization of 20% of olivine from the primary magma calculate by the COMAGMAT program **[6]**); (5) weighted mean composition of the layered series of the Central pluton **[2]**; (6) chondrite composition **[8]**; (7) N-MORB composition **[9]**; (8) primitive mantle composition **[9]**; (9) composition of the N-MORB source (MORBMA) **[10]**; (10) bulk composition of the Vourinos ophiolite complex, Greece **[11]**; (11) composition of the hypothetical source of the mantle-derived primary melt of the Central pluton; (12) composition of the primary melt deduced from modeling of partial melting of the source (11) by the MELTS program **[12]** at 1600^{o} C, 25 kbar, 0.1 wt % H_2O in the source, and QFM buffer; and (13) composition of the primary melt deduced from modeling of partial melting of the primitive mantle source (8) by the MELTS program **[12]** at 1600^{o} C, 25 kbar, 0.1 wt % H_2O in the source, and QFM buffer. Mg # = 100Mg/(Mg + Fe). FeO is total iron.

Fig. 4. The layered intrusion formation according to modeling results. (a, b) Crystallization of the primary model melt for the Central pluton; (c, d) crystallization of the parental melt for the Central pluton. Modeling was carried out by the COMAGMAT 3.5 program **[6]** at 1 kbar, QFM buffer, 0.5 wt % H_2O in the melt, and degree of crystallization of 80%. The sequence of mineral formation is shown in panels a and b versus the degree of crystallization (F) and in panels c and d as a function of decreasing temperature (T).
(1) olivine, (2) plagioclase, (3) clinopyroxene, and (4) orthopyroxene.

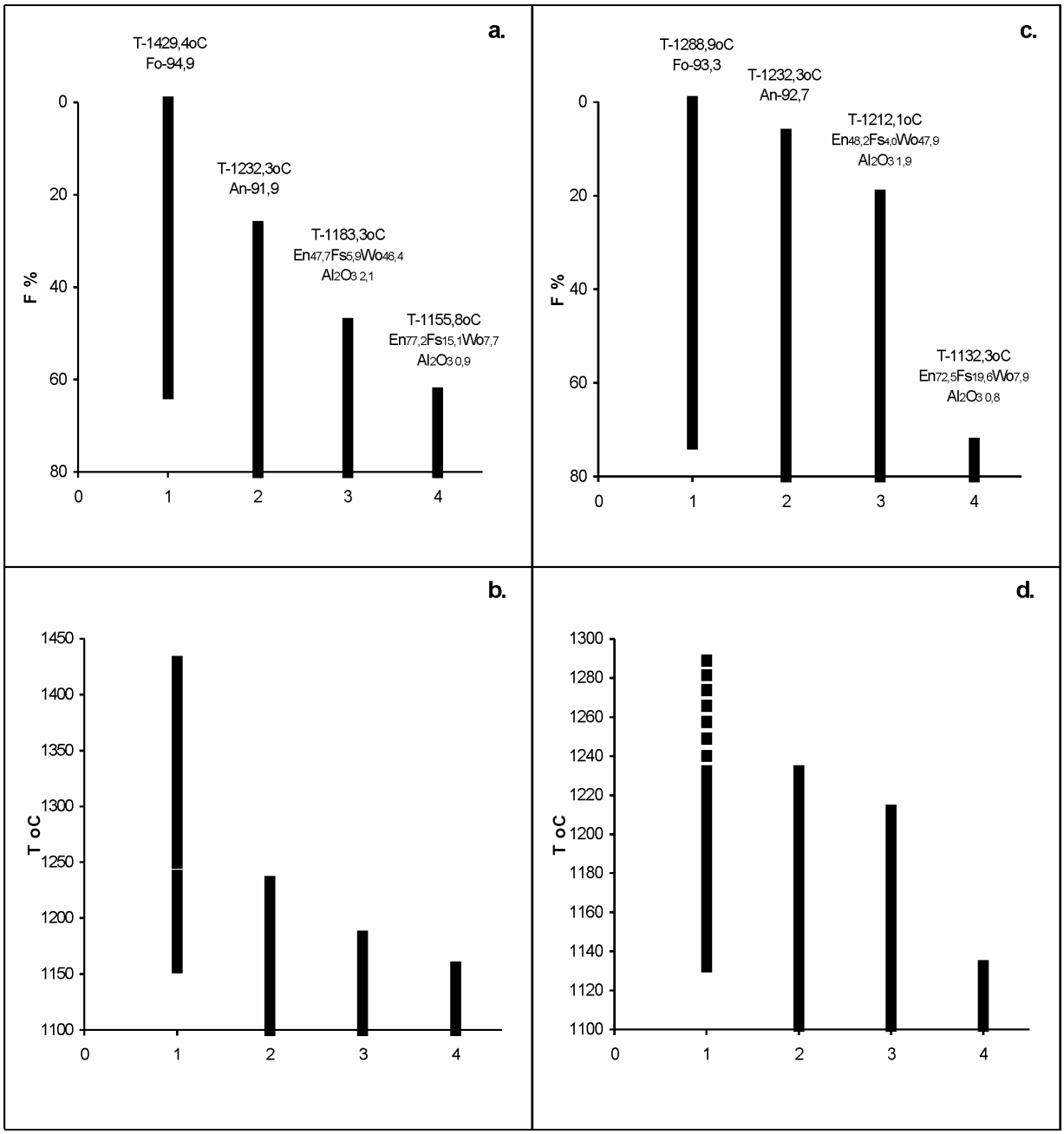

Fig. 5. Variation of major oxides and trace elements versus MgO, wt %.(1) Rocks of the layered series of the Central pluton; Sample I-2038 from the marginal facies is shown by the large symbol; (2) calculated compositions of cumulus phases; crystallization of the model primary magma for the Central pluton was modeled by the COMAGMAT 3.5 program **[6]** at 1 kbar, QFM buffer, and 0.5 wt % H_2O in the melt; (3) composition of the model primary melt for of Central pluton; (4) weighted mean composition of the layered series of the Central pluton **[2]**; (5) composition of the marginal facies of the Central pluton (Sample I-2038); and (6) model residual melt after crystallization of 20% olivine.

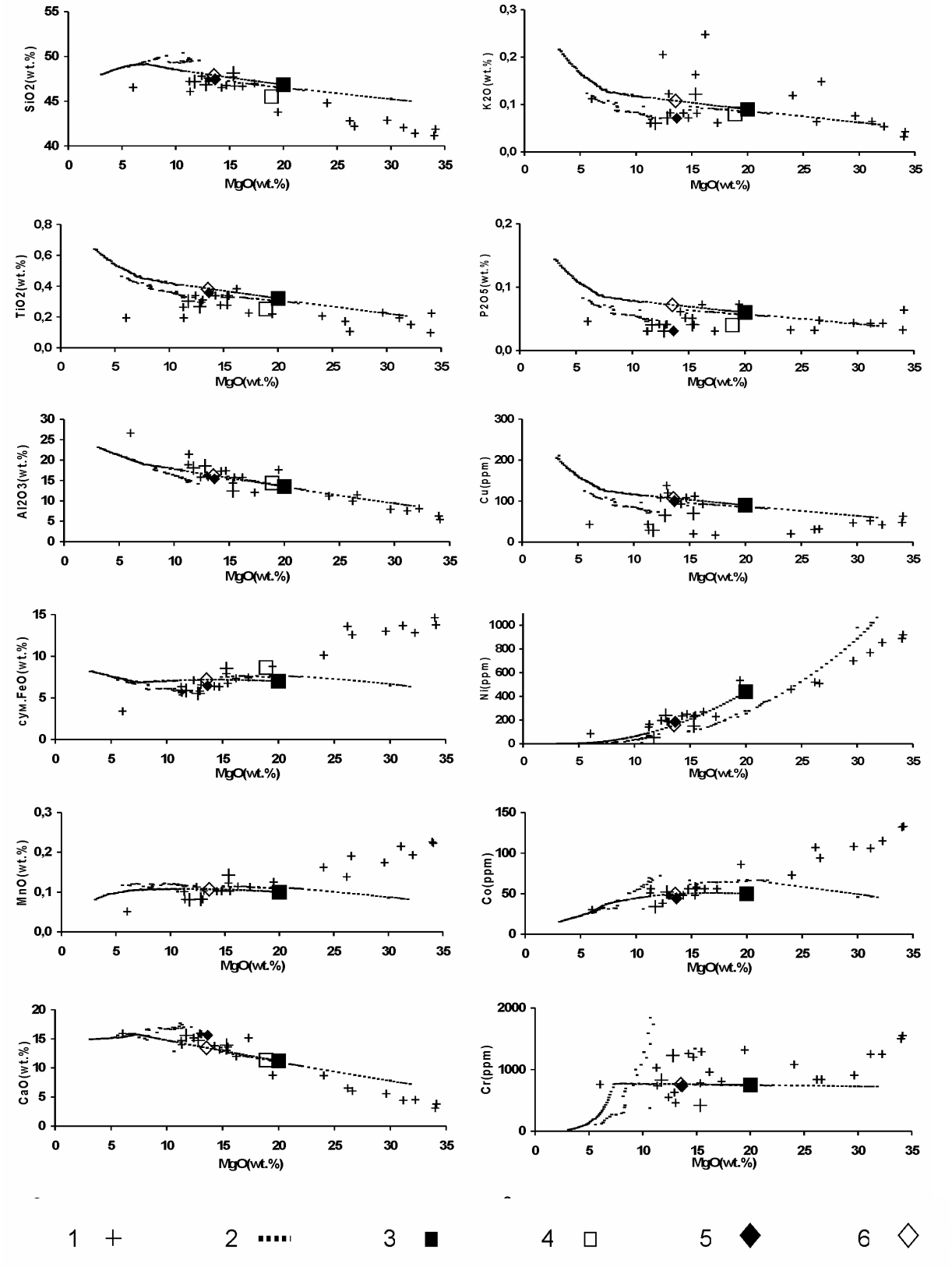
SiO2(wt.%)
MgO(wt.%)
K2O(wt.%)
TiO2(wt.%)
P2O5(wt.%)
Al2O3(wt.%)
Cu(ppm)
сум.FeO(wt.%)
Ni(ppm)
MnO(wt.%)
Co(ppm)
CaO(wt.%)
Cr(ppm)
1
2
3
4
5
6

Fig. 6. Fractional crystallization of the Central pluton according to modeling.
(1) Rocks of the layered series; Sample I-2038 is shown by the large symbol; (2) composition of residual melts calculated by the COMAGMAT 3.5 program [6] for model primary melt crystallization at 1 kbar, QFM buffer, and 0.5 wt % H_2O in the melt; (3) composition of residual melts calculated by the MELTS program **[12]** for model primary melt crystallization at 1 kbar, QFM buffer, and 0.5 wt % H_2O in the melt; (4) composition of the model primary melt for the Central pluton; (5) weighted mean composition of the layered series of the Central pluton **[2]**; (6) composition of the marginal facies of the Central pluton (Sample I-2038); (7) Vendian and Cambrian volcanics of the Lake Zone, western Mongolia **[16]**; the composition of the high-alumina basalt from the Lower Cambrian Irbitei sequence, eastern Tannu-Ola, Tuva **[1]** is shown by the large symbol.

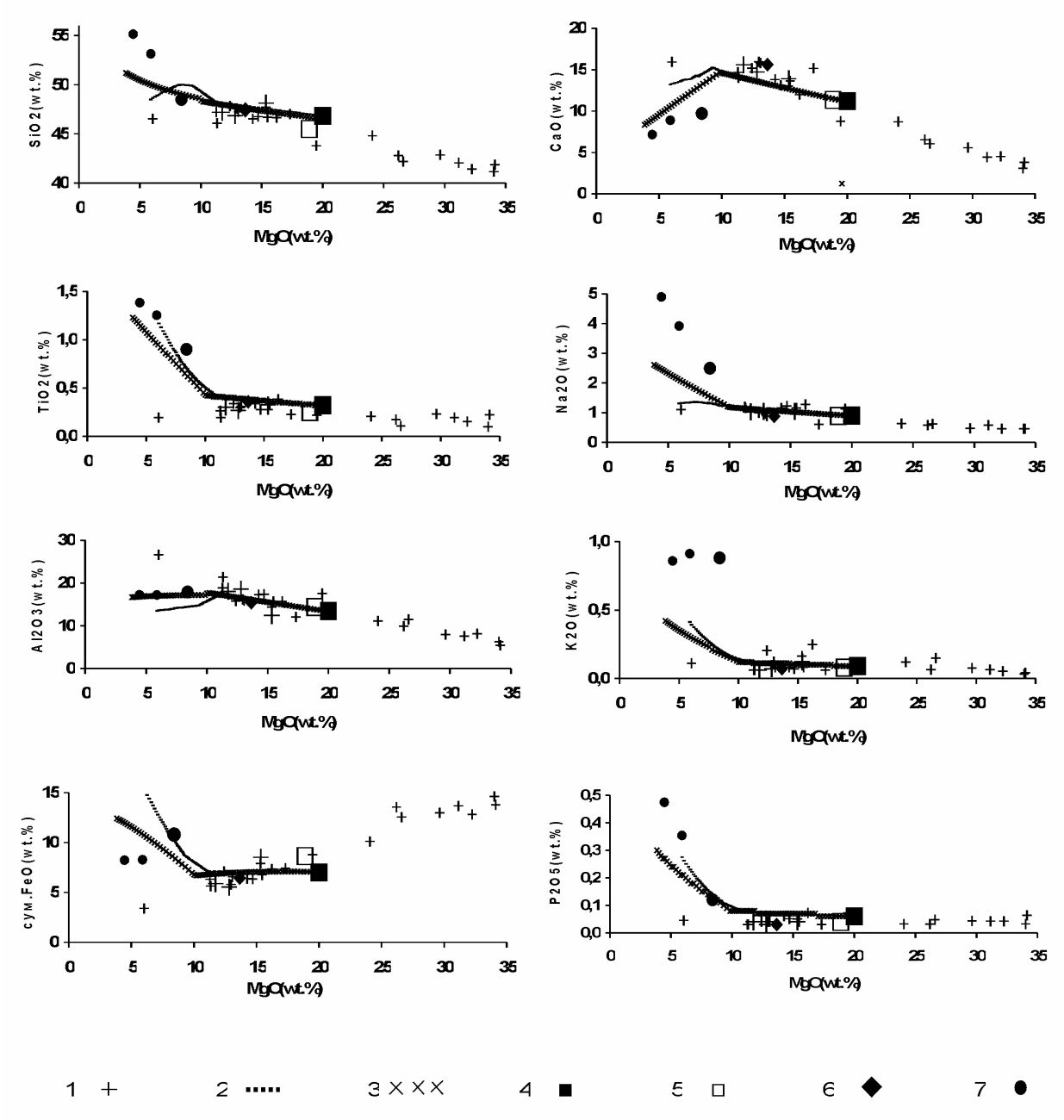

GEOCHEMISTRY OF THE CENTRAL PLUTON

According to the classification **[17, 18]**, the composition of the model primary melt of the Central pluton and the weighted mean composition of the layered series correspond to picrite. The normative olivine contents of the primary melt and the weighted mean composition are 33.1 wt % (Mg# =83.6) and 37.7 wt % (Mg# =79.6), respectively **(Table 6)**. The compositional evolution of the Central pluton follows the general trend of mafic rock fractionation on the AFM diagram **(Fig. 7)**. The compositions of the most melanocratic rocks of the Central pluton are confined to the compositional fields of the respective rocks from the young Mariana and Tonga-Kermadec island arcs **[19]** and melanocratic cumulates of the Skaergaard pluton **[20]**. The compositions of highly evolved rocks from the Central pluton extend along the trend of island-arc rocks. The short evolution trend for the rocks of the Central pluton points to the limited degree of parental melt fractionation, which is typical of one-phase intrusions.

All rocks of the Central pluton show similar chondrite-normalized **[8]** REE patterns **(Fig. 8a-c)** with unfractionated distribution of LREE and intermediate REE and normalized contents of about 2 in the plagiocalse peridotite and 3-5 in the olivine gabbro. All rocks are slightly depleted in HREE: 1.2 in the plagioclase peridotite and 2-3 in the olivine gabbro. The chondrite-normalized **[8]** $(La/Yb)_{ch}$ ratio in the rocks of the layered series is within 1.60-1.91 (1.70, on average). The $(La/Sm)_{ch}$ ratio varies from 0.86 to 1.35 (1.03, on average), and $(Sm/Yb)_{ch}$, from 1.42 to 1.86 (1.67, on average) **(Table 7)**. The REE distribution patterns exhibit a nearly parallel shift to higher contents from the basal unit of plagioclase peridotite to the olivine gabbro of layered series. The olivine gabbro displays a more pronounced Eu maximum than the rocks of the marginal zone and the plagioclase peridotite owing to plagioclase accumulation in this rock **[21]**. The Eu/Eu* ratio varies from 1.02 in the marginal facies (Sample I-2038) to 1.16 in the most evolved olivine gabbro (Sample I-1989) suggesting a slight positive Eu anomaly (Eu/Eu* > 1) in the rocks of the layered series **(Table 7)**. The REE distribution normalized to PM and N-MORB **[9] (Figs. 8b and 8c)** also exhibits extremely low REE contents in the rocks of the Central pluton. Only U and Th contents are higher than those of N-MORB, whereas the normalized contents of other elements vary from 0.08 to 0.60. U and Th contents are also higher than in PM (by a factor of 14,29), and the total of REE is 0.93-2.78 PM units. In addition to the U and Th maxima, the rocks of the Central pluton are distinguished by distinct negative Ta and Hf anomalies expressed in all rocks and a slight deficit in Ti, which is observed in the marginal facies and layered series except for the basal plagioclase peridotite unit. The pronounced depletion of rocks in HREE is observed in the chondrite- and N-MORB-normalized REE patterns. This geochemical signature could be inherited from the garnet-bearing source **[22]**. The geochemical characteristics of rocks from the Central pluton are typical of subduction-related magmas. The low Ti content (0.10-0.38 wt %), high chondrite- and N-MORB-normalized LILE/HFSE ratios: $(U/Th)_{N\text{-}MORB}$ = 1.70-3.83 and $(U/Th)_{PM}$ = 2.37-5.33; and high LILE/REE ratios: $(U/La)_{N\text{-}MORB}$ = 7.6-15 and $(U/La)_{PM}$ = 3.76-7.51 are indicative features. The elevated U and Th contents and slight enrichment in LREE with $(La/Yb)_{ch}$ = 1.60-1.91 and $(La/Yb)_{N\text{-}MORB}$ = 2.89-3.45 **(Figs. 8a and 8b; Table 7)** along with the ubiquituous Ta minimum bring the rocks of the Central pluton together with the island-arc tholeiitic series.

The REE patterns of volcanics from the Lake Zone **(Figs. 8d-8f)** are similar in many respects to those of the rocks of the Central pluton. The REE spectra are nearly parallel to one another. The common depletion in HREE is especially notable: $(Eu/Yb)_{ch}$ of 1.61-1.88 for the

plutonic rocks and 1.64-1.67 for the volcanic rocks. This similarity implies that the magma sources for both series were localized in the garnet stability field. The occurrence of garnet in the mantle source of volcanics is also supported by a relatively constant Yb content (2.27-2.36 ppm) and widely varying LREE (10.6-12.8 ppm La) and especially Th (0.78-5.66 ppm) contents **[21]**. In general, the volcanic rocks are characterized by higher REE contents (REE sum of 74.66-75.53 ppm) than the plutonic rocks (REE sum of 5.32-11.50). It should be noted that the volcanics are 8-18 times richer in LREE, and only 4-8 times richer in HREE. The volcanic and plutonic rocks are depleted in Hf. Ta and Nb minima are distinct specific features of the volcanic rocks from the Lake Zone and of the Central pluton **[16]**. These geochemical signatures indicate that the volcanics are related to the subduction zones. The geochemical similarity between the volcanic and plutonic rocks suggest the existence of a common garnet-bearing mantle source.

Fig. 7. Variation of rock compositions plotted on the AFM diagram.
(1) Rocks of the layered series; Sample I-2038 is shown by the large symbol; (2) model primary melt of the Central pluton; (3) weighted mean composition of the layered series of the Central pluton **[2]**; (4) trend of the cumulus phase compositions for the crystallization of the model primary magma of the Central pluton modeled by the COMAGMAT 3.5 program **[6]** at 1 kbar, QFM buffer, and 0.5 wt % H_2O in the melt; (5) composition of residual melts calculated by the MELTS program **[12]** for model primary melt crystallization at 1 kbar, QFM buffer, and 0.5 wt % H_2O in the melt; (6) model composition of the primary melt calculated by the MELTS program **[12]** for partial melting of the hypothetical mantle source of the Central pluton at T = 1600^{o}C, P = 25 kbar, QFM buffer, and 0.1 wt % H_2O in the source; the composition of the hypothetical mantle source with Fo-92.06 is shown by the large symbol; (7) Vendian and Cambrian volcanics of the Lake Zone, western Mongolia **[16]**; composition of high-alumina basalt from the Lower Cambrian Irbitei sequence, eastern Tannu-Ola, Tuva **[1]** is shown by the large symbol; (8) Tonga-Kermadec island-arc trend **[19]**; (9) Mariana island-arc trend **[19]**; (10) residual melts of the Skaergaard plutons **[20]**; (11) melanocratic cumulate of the Skaergaard pluton; the parental magma composition of the Skaergaard pluton **[20]** is shown by the large symbol.

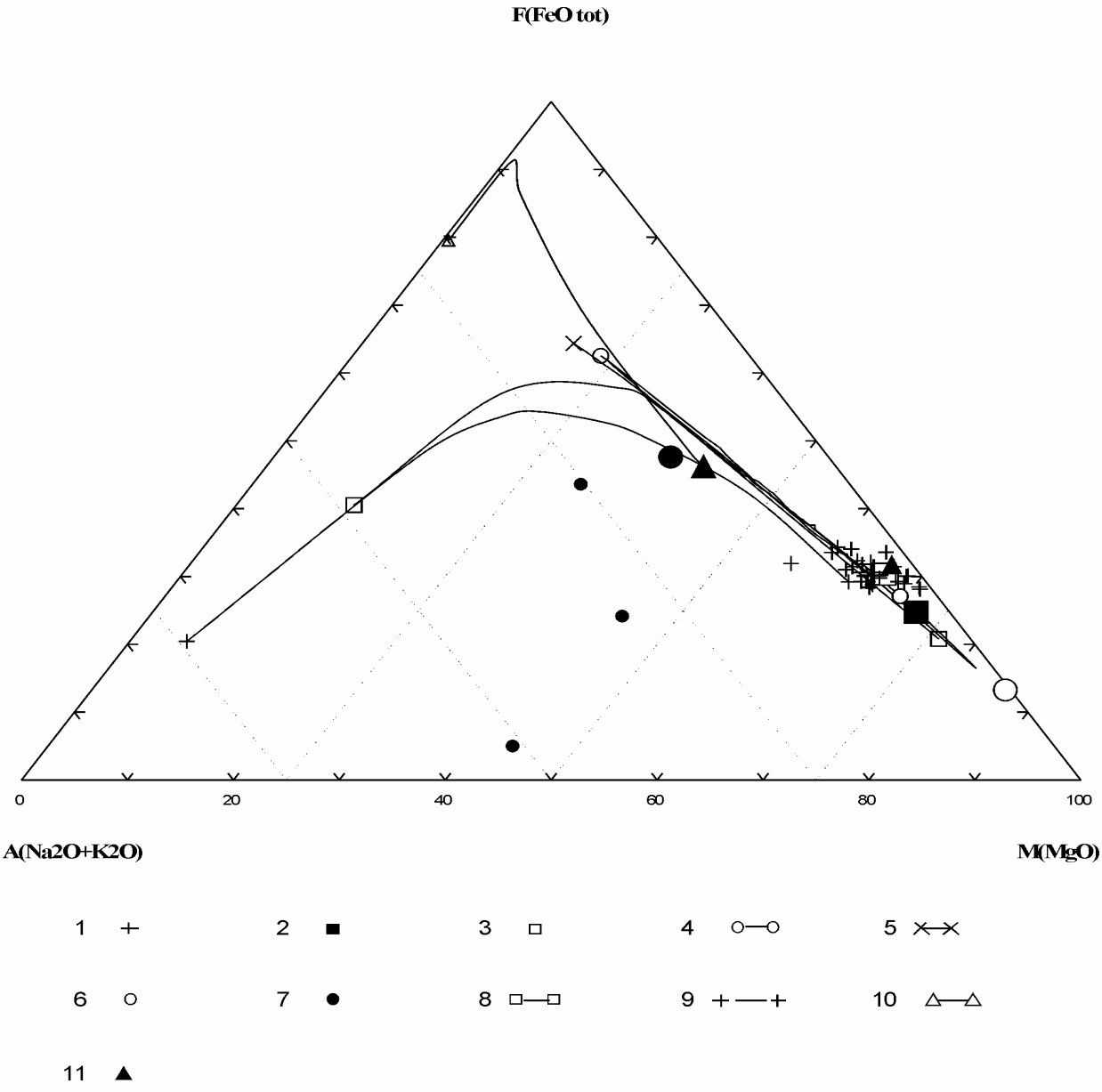

Fig. 8. Normalized REE patterns in (a-c) the gabbroids of the Central pluton and (d-f) Vendian-Cambrian volcanic rocks of the Lake Zone in comparison with the gabbroids of the Central pluton.
(1) Sample I-1984; (2) Sample I-2038; (3) Sample I-2045; (4) Sample 1989; (5) model primary melt of the Central pluton; Vendian-Cambrian volcanic rocks of the Lake Zone, western Mongolia **[16]**: (6) Sample GU-4898/5 and (7) Sample GU-4998/4; (8) N-MORB mantle source (MORBMA) **[10]**; and (9) primitive mantle (PM) **[9]**. REE compositions were normalized to C1 chondrite **[8]**, N-MORB **[9]**, and PM **[9]**.

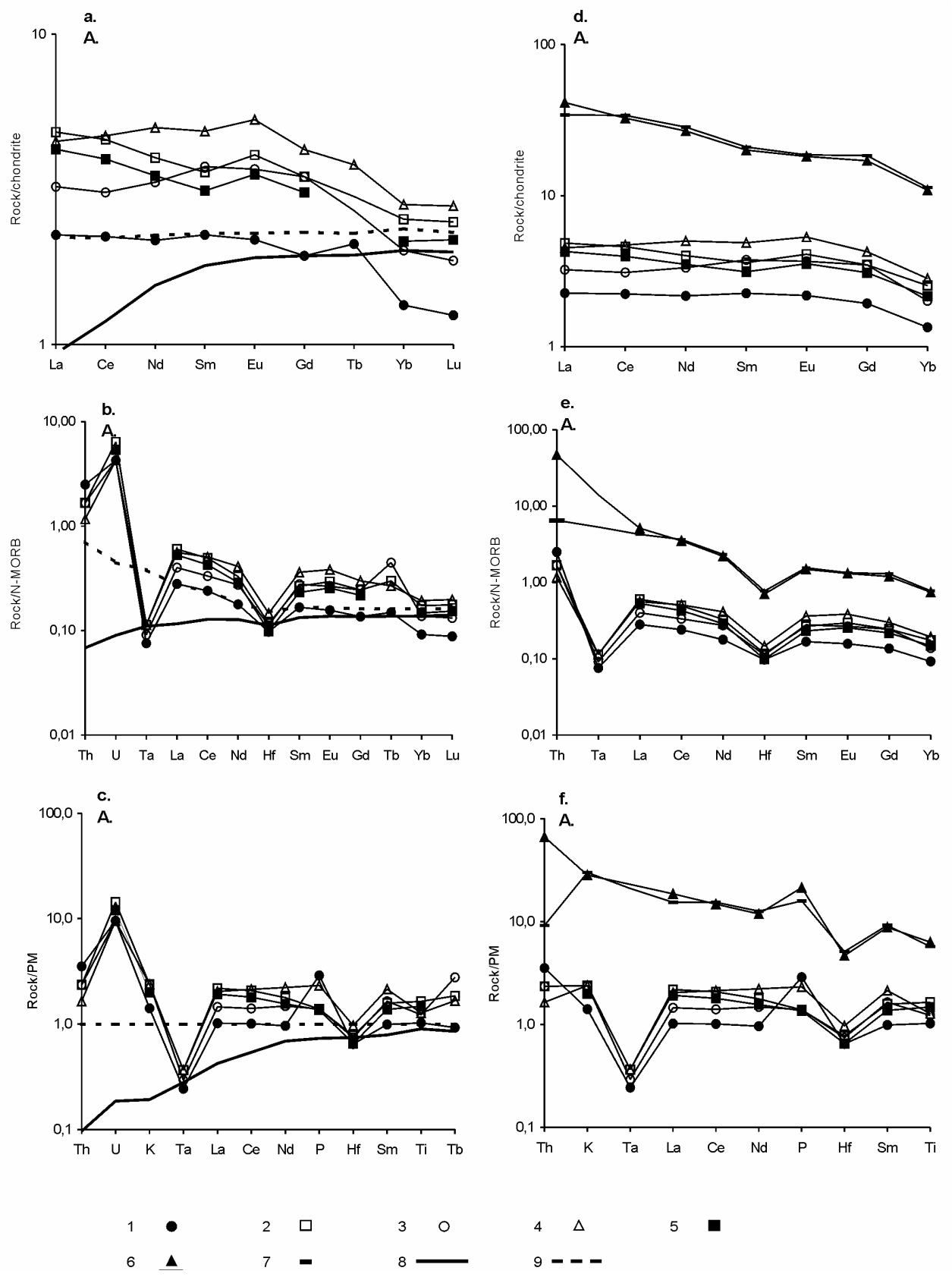
a.
A.
Rock/chondrite
10
1
La Ce Nd Sm Eu Gd Tb Yb Lu
d.
A.
Rock/chondrite
100
10
1
La Ce Nd Sm Eu Gd Yb
b.
A.
Rock/N-MORB
10,00
1,00
0,10
0,01
Th U Ta La Ce Nd Hf Sm Eu Gd Tb Yb Lu
e.
A.
Rock/N-MORB
100,00
10,00
1,00
0,10
0,01
Th Ta La Ce Nd Hf Sm Eu Gd Yb
c.
A.
Rock/PM
100,0
10,0
1,0
0,1
Th U K Ta La Ce Nd P Hf Sm Ti Tb
f.
A.
Rock/PM
100,0
10,0
1,0
0,1
Th K Ta La Ce Nd P Hf Sm Ti
1
2
3
4
5
6
7
8
9

Table 7. The chemical composition of rocks from the Central pluton (major elements are in wt %, trace elements, in ppm)

Sample	И2036	И1962	8430	И1985	И1984	8434	8433	И2028	И1989	И1990	И1987	И2045	И2038
Component	1	2	3	4	5	6	7	8	9	10	11	12	13
SiO_2	39,09	38,15	39,36	38,55	39,37	39,81	40,13	41,35	45,57	45,74	45,42	45,70	46,52
TiO_2	0,18	0,09	0,21	0,14	0,21	0,10	0,16	0,19	0,27	0,33	0,33	0,26	0,35
Al_2O_3	7,04	5,81	7,30	7,55	5,10	10,84	9,32	10,31	16,92	15,41	16,86	18,11	15,09
Fe_2O_3	5,71	6,27	6,54	5,21	4,65	3,80	5,75	5,82	1,64	2,17	2,04	1,74	1,92
FeO	7,58	7,91	6,04	7,24	8,77	8,44	7,55	4,10	4,70	4,66	4,41	3,84	4,59
FeO total	12,72	13,55	11,93	11,93	12,96	11,86	12,73	9,34	6,18	6,61	6,25	5,41	6,32
MnO	0,20	0,21	0,16	0,18	0,21	0,18	0,13	0,15	0,10	0,10	0,10	0,08	0,10
MgO	28,97	31,54	27,22	30,01	32,09	25,11	24,56	22,21	14,33	15,15	13,92	12,49	13,39
CaO	4,13	2,86	5,12	4,20	3,57	5,70	6,12	8,02	12,78	13,36	13,49	14,36	15,32
Na_2O	0,54	0,43	0,43	0,43	0,43	0,59	0,54	0,59	1,19	1,13	1,13	1,02	0,86
K_2O	0,06	0,03	0,07	0,05	0,04	0,14	0,06	0,11	0,07	0,08	0,08	0,07	0,07
P_2O_5	0,04	0,03	0,04	0,04	0,06	0,05	0,03	0,03	0,05	0,04	0,06	0,03	0,03
L.O.I.	5,77	6,51	6,98	5,98	4,79	4,68	5,15	6,64	1,73	1,58	1,74	1,79	1,38
Total	99,31	99,84	99,47	99,58	99,29	99,43	99,50	99,52	99,35	99,75	99,58	99,49	99,62
Fe3+/Fe2+	0,75	0,79	1,08	0,72	0,53	0,45	0,76	1,42	0,35	0,47	0,46	0,45	0,42
Mg #	80,24	80,58	80,27	81,77	81,54	79,06	77,48	80,92	80,53	80,33	79,89	80,47	79,07
Cu	52	48	47	42	63	32	31	20	108	112	93	65	100
Ni	770	890	700	855	920	510	520	460	250	240	235	240	185
Co	106	132	108	115	133	94	107	73	56	58	48	52	44
Cr	1250	1500	910	1250	1550	840	840	1080	1200	1290	1260	1230	730
La					0,70				1,40			1,00	1,50
Ce					1,80				3,80			2,50	3,70
Nd					1,30				3,00			2,00	2,40
Sm					0,44				0,95			0,73	0,70
Eu					0,16				0,39			0,27	0,30
Gd					0,50				1,10			0,90	0,90
Tb					0,10				0,18			0,30	0,20
Yb					0,28				0,59			0,42	0,53
Lu					0,04				0,09			0,06	0,08
Eu /Eu*					1,04				1,16			1,02	1,16
Hf					0,20				0,30			0,23	0,24
Ta					0,01				0,02			0,01	0,02
Th					0,30				0,14			0,20	0,20
U					0,20				0,20			0,20	0,30
(La/Yb)ch					1,69				1,60			1,61	1,91
(La/Sm)ch					1,00				0,93			0,86	1,35
(Sm/Yb)ch					1,68				1,73			1,86	1,42

Sample	И2027	8428	И2037	И1988	И2030	8432	8427	8426	И2035	8436	И1964	И2026
Component	14	15	16	17	18	19	20	21	22	23	24	25
SiO_2	46,76	46,57	45,79	41,97	45,82	46,53	46,63	45,23	45,17	45,62	46,79	47,34
TiO_2	0,27	0,29	0,30	0,21	0,22	0,33	0,26	0,19	0,37	0,19	0,30	0,32
Al_2O_3	14,10	15,84	15,41	16,85	11,76	15,40	18,63	21,03	15,24	26,09	17,92	12,21
Fe_2O_3	1,97	1,64	2,28	2,69	1,89	2,51	1,89	1,42	1,88	1,69	1,70	2,44
FeO	5,97	4,21	4,30	5,99	5,54	4,66	4,55	4,26	5,41	1,81	4,30	6,19
FeO total	7,74	5,69	6,35	8,41	7,24	6,92	6,25	5,54	7,10	3,33	5,83	8,39
MnO	0,12	0,08	0,10	0,12	0,11	0,11	0,10	0,08	0,11	0,05	0,08	0,14
MgO	15,03	12,68	12,67	18,67	16,88	12,07	11,14	11,13	15,69	5,92	11,64	15,09

CaO	12,77	15,61	15,33	8,40	14,77	14,77	14,49	13,75	11,59	15,61	15,46	13,68
Na_2O	1,02	0,95	0,86	1,08	0,59	0,97	1,19	1,13	1,24	1,08	1,02	1,02
K_2O	0,16	0,12	0,08	0,08	0,06	0,20	0,06	0,06	0,24	0,11	0,06	0,12
P_2O_5	0,05	0,04	0,04	0,07	0,03	0,04	0,03	0,03	0,07	0,05	0,04	0,04
L.O.I.	1,18	1,61	2,36	3,26	1,69	2,03	1,18	1,10	2,31	1,28	1,37	1,57
Total	99,40	99,64	99,52	99,39	99,36	99,62	100,15	99,41	99,32	99,49	100,68	100,16
Fe3+/Fe2+	0,33	0,39	0,53	0,45	0,34	0,54	0,42	0,33	0,35	0,93	0,40	0,39
Mg #	77,58	79,90	78,05	79,83	80,61	75,67	76,06	78,18	79,75	76,01	78,07	76,24
Cu	20	138	120	320	17	108	43	29	93	43	29	70
Ni	230	190	186	535	230	196	142	164	270	86	52	150
Co	48	48	48	86	56	38	51	56	56	30	34	56
Cr	780	630	460	1320	810	550	1030	740	960	760	830	420

Note: 1 - Pl-beraing dunite, 2, 3 - plagioclase peridotite, 4 - wehrlite, 5 - troctolite, 6-8 - melanogabbro, 9-11, 14-21 - olivine gabbro, 12, 22 - amphibolized olivine gabbro, 13, 24, 25 - olivine gabbro of marginal facies, 23 - anorthosite. Eu/Eu* is the ratio of the measured chondrite-normalized Eu content to the Eu* value interpolated between chondrite-normalized Sm and Gd contents.

PRIMARY MAGMA AND MANTLE SOURCE COMPOSITIONS

In this work, we attempted to specify, based on geochemical and petrogenetic relationships, some typical features of the mantle source and primary magma of the Central pluton and possible conditions of melt generation. Basic rocks similar to those of the Central pluton were previously considered to be products of melting of the depleted mantle **[2]**. As is known **[23, 24]**, HFSE (Ta, Hf, Ti, etc.) and HREE are immobile in the process of subduction-related oceanic plate dehydration and their contents are inherited from mantle composition before the subduction. In the case of the Central pluton, the mantle component was similar to the depleted mantle source before the enrichment in mobile elements **(Fig. 8f)**.

The presence of garnet in the residue after primary melt generation provides important constraints on the depth of magma generation. Dostal **[22]** proposed a method to determine the type of mantle source from REE contents in the melt equilibrated with this source as a function of the degree of partial melting; the equations derived by Shaw **[25]** were used for this purpose.

The composition of liquid formed upon batch melting, when the liquid phase remains in equilibrium with solids, is calculated from the proportions of mineral phases in the residue. The concentration of a given element, i, in the melt (C_i^l) is related to its concentration in the initial solid matter C_i^0 as **[25]**

$C_i^l/C_i^0 = 1/[D_i^0 + F(1 - D_i^0)]$, (1)

where F is the melt fraction; D_i^0 is the bulk solid/liquid partition coefficient for a given

$$D_i^o = \sum_{j=1}^{N} K_i^j x_i^s$$

element, i:

where x_i^s is the fraction of a given mineral, i, in the solid residue (s) and K_i^j is the partition coefficient of a given element, i, between the mineral, i, and melt.

The set of mineral phases and their proportions change with increasing degree of melting. Although these changes occur as discrete steps, the linear approximation derived by Shaw allows the description of general variations in the melt composition. In the case of equilibrium partial melting **[25]**:

$D_i = (D_i^0 - P_iF)/(1 - F)$; (2)

$$P_i = \sum_{j=1}^{N} K_i^j p_i$$

where P_i is the bulk partition coefficient of a given element, i, for minerals consumed by melting and p_i is the fraction of a given phase, i, in melt.

The concentration C_i^1 of a given element, i, in the melt is determined from equations (1) and (2) **[25]**:

$C_i^1 / C_i^0 = 1/[D_i^0 + F(1 - P_i)]$. (3)

Given the source mineralogy, proportions of phases consumed by melting **[22]**, and partition coefficients between these phases and melt **(Table 8)**, the REE content of melt equilibrated with a mantle source can be calculated for any F value. In our case, the inferred N-MORB source (MORBMA) **[10]** of the Central pluton **(Table 6)** was modeled for three mineral assemblages: garnet lherzolite, quartz eclogite, and spinel lherzolite **(Table 9)**. The calculated chondrite-normalized **[8]** REE contents in the melts equilibrated with mantle sources were compared with the REE patterns of the primary melt of the Central pluton **(Fig. 9)**. The comparison has shown that the REE distribution patterns of the primary melt are consistent with the garnet lherzolite source.

As follows from the aforesaid, the primary melt of the Central pluton is picritic in composition and characterized by extremely low REE contents and relatively high Ni content in comparison to MORB: 8.44 ppm REE and 440 ppm Ni in the primary melt against 28.81 ppm REE and 177 ppm Ni in N-MORB **[9] (Table 6)**. This geochemical signature is characteristic of a primary picritic melt formed at high pressure and temperature through garnet lherzolite melting. The estimated composition of the primary mantle melt brought in equilibrium with the inferred garnet-bearing source is a key point in the evaluation of the extent of fractionation of the primary melt of the Central pluton during its ascent. The calculation method was proposed by Hanson and Langmuir **[31]**, who used the relationships between MgO and FeO for the primary melt discrimination. The method includes the calculation of MgO and FeO contents in melt in equilibrium with the given mantle source at the lowest and highest degrees of melting and, thus, specifies the primary melts at certain P-T conditions. According to experimental data **[32]**, garnet is stable under anhydrous conditions above 27 kbar. The alumina content of the primary melt generated in the stability field of garnet peridotite decreases with increasing total pressure, and this relationship can serve as an indicator for the depth of melting **[33]**. The Al_2O_3 content of picrite produced at 28 kbar is 13-14 wt % **[34]**. At a pressure higher than 30 kbar, the melts contain <13 wt % Al_2O_3 **[33]**. According to these data, the Al_2O_3 content of the primary melt of the Central pluton (13.5 wt %) corresponds to its generation at a lithostatic pressure of 28-30 kbar under anhydrous conditions. Island-arc systems are usually water-bearing, and, thus, the melting therein occurs at lower pressure relative to the anhydrous system under the same composition.

The method of Hanson and Langmuir **[31]** was used for the calculation of MgO and FeO contents in a primary melt in equilibrium with a hypothetical garnet-bearing mantle source with Fo-92.06 within a temperature range of 1525-1850°C **(Fig. 10; Table 6)** for the limiting case of anhydrous melting at 30 kbar. The experimental data on the olivine/melt partition coefficients in

high-Mg systems at a pressure of 30 kbar are given in **[35, 36]**. The composition of the primary melt of the Central pluton falls into the field of primary mantle melts with Fo-92.06 bounded by lines corresponding to the highest (F_{max}) and lowest (F_{min} = 0) degrees of melting **(Fig. 10)**. The line of melt composition at P = 30 kbar and F = 28% goes through the composition of the primary melt of the Central pluton at a temperature of ~1650^{o}C. This implies that such composition could be a primary magma. It should be noted that this method of estimation of the primary melt composition is very approximate, because the linear relationship between parameters is valid only for small segments. In general, melt composition changes step-wise increasing the uncertainty of calculations. This made to use other models of partial melting. The MELTS program **[12]** is based on the minimization of the Gibbs potential and eliminates the issue of nonlinear integral trends. As was shown in **[37]**, the results of thermodynamic computation by MELTS are in good agreement with experimental data. However, a systematic discrepancy exists between the calculated composition of partial melts and experimental compositions for some oxides. For example, the calculated MgO content is overestimated in comparison with experimental data by 2-3 wt % for fertile peridotite and by 3.5-4.5 wt % for depleted peridotite depending on the degree of partial melting. On the contrary, SiO_2 content is systematically underestimated by 3-4 wt % in comparison with experimental data because of the shrinkage of the olivine stability field and expansion of the orthopyroxene field relative to experimental results. The calculated melt compositions may differ significantly from compositions obtained in experiments at low degrees of partial melting (F). The calculated CaO content of the melts derived from depleted peridotite at F < 0.1 is higher by 0.5-1.5 wt % than CaO in experimental melts. The discrepancy reaches 1-2 wt % for fertile peridotite at F < 0.2. The Al_2O_3 content of model melts is lower than that of experimental melts by 0-1.3 wt % for fertile peridotite and by 1.5-3.0 wt % for depleted peridotite. The calculated FeO content for depleted peridotite is systematically overestimated by 1.5-3.0 wt %. A model primary melt was calculated using the MELTS program for equilibrium with a hypothetical mantle source with Fo-92.06 at 25 kbar, QFM buffer, and 0.1 wt % of water in the source, which is equal to the mean water content of the upper mantle **[32]**. Taking into account the systematic errors of calculations, the model mantle melt is identical to the primary melt of the Central pluton **(Table 6)**. The Vourinos ophiolite complex in Greece **[11]** is most similar to the inferred mantle source of the Central pluton **(Fig. 10; Table 6)**. The batch melting of the primitive mantle **[9]** under the same conditions yields melts containing more than 6 mol % (11.15 wt %) FeO **(Table 6)**. This rules out the possibility of parental magma generation in fertile mantle sources. The coeval subduction-related high-alumina volcanics of the Lake Zone can be comagmatic to the rocks of the Central pluton, if the effects of contamination or magma mixing are taken into account. In any case, the volcanic and plutonic rocks could be derived from a common garnet-bearing mantle source. Some high-alumina layered basic plutons of the Lake Zone also could be shallow-seated comagmatic counterparts of these volcanics. Most likely, the Central pluton is a hypabyssal analogue of primitive high-Mg island-arc basalts with high Ni and Cr contents, which are often associated with high-alumina island-arc basalts **[23]**.

Table 8. The calculated bulk partition coefficients: residue/liquid (D_0) and minerals consumed by melting/liquid (P) for various mantle sources

Mineral/liquid partition coefficient	La	Ce	Nd	Sm	Eu	Gd	Yb	Lu	U	Hf
Ol / liq [26]	0,007	0,006	0,006	0,007	0,007	0,010	0,049	0,045		

Ol / liq [27]									0,002	0,013
Opx / liq [28]	0,020	0,020	0,030	0,050	0,050	0,090	0,340	0,420		
Cpx / liq [26]	0,056	0,092	0,230	0,445	0,474	0,556	0,542	0,506		
Grt / liq [29]	0,001	0,007	0,026	0,102	0,243	0,680	6,167	6,950		
Sp / liq [30]	0,001	0,001	0,001	0,001	0,001	0,001	0,005	0,005		
Garnet lherzolite										
Mineral contents in the source: Ol-60%,Opx-20%,Cpx-10%,Grt-10%										
Mineral contents in the melt: Ol-40%,Opx-15%,Cpx-25%,Grt-20%										
Coefficient	**La**	**Ce**	**Nd**	**Sm**	**Eu**	**Gd**	**Yb**	**Lu**		
Do	0,016	0,021	0,042	0,083	0,103	0,177	0,922	1,028		
P	0,024	0,036	0,083	0,170	0,213	0,351	1,727	1,917		
Eclogite										
Mineral contents in the source: Cpx-50%,Grt-50%										
Mineral contents in the melt: Cpx-80%,Grt-20%										
Coefficient	**La**	**Ce**	**Nd**	**Sm**	**Eu**	**Gd**	**Yb**	**Lu**		
Do	0,029	0,050	0,128	0,274	0,359	0,618	3,355	3,728		
P	0,045	0,075	0,189	0,376	0,428	0,581	1,667	1,795		
Spinel lherzolite										
Mineral contents in the source: Ol-55%,Opx-15%,Cpx-25%,Sp-5%										
Mineral contents in the melt: Ol-35%,Opx-15%,Cpx-50%,Sp-0%										
Coefficient	**La**	**Ce**	**Nd**	**Sm**	**Eu**	**Gd**	**Yb**	**Lu**		
Do	0,021	0,030	0,066	0,123	0,130	0,159	0,216	0,217		
P	0,033	0,051	0,122	0,232	0,247	0,295	0,339	0,332		

Note: The mineral compositions of sources and proportions of minerals entering melts are given after **[22]**. (Ol) Olivine, (Opx) orthopyroxene, (Cpx) clinopyroxene, (Grt) garnet, and (Sp) spinel.

Table 9. The calculated REE content (ppm) of melt as a function of the degree of partial melting (F)

Garnet lherzolite								
F	**La**	**Ce**	**Nd**	**Sm**	**Eu**	**Gd**	**Yb**	**Lu**
F=0,005	13,59	37,18	19,89	4,03	1,30	2,77	0,46	0,06
F=0,1	2,54	8,18	6,95	2,11	0,77	2,07	0,49	0,07
F=0,2	1,37	4,49	4,12	1,41	0,54	1,63	0,54	0,08
F=0,3	0,94	3,09	2,93	1,06	0,41	1,34	0,60	0,08
F=0,4	0,71	2,36	2,28	0,84	0,33	1,14	0,67	0,10
F=0,5	0,57	1,91	1,86	0,70	0,28	1,00	0,75	0,11
F=1	0,29	0,97	0,97	0,38	0,16	0,61	2,16	0,58
Eclogite								
F	**La**	**Ce**	**Nd**	**Sm**	**Eu**	**Gd**	**Yb**	**Lu**
F=0,005	7,44	14,99	5,90	1,06	0,32	0,67	0,10	0,01
F=0,1	2,23	6,30	3,95	0,90	0,29	0,66	0,12	0,02
F=0,2	1,28	3,92	2,94	0,78	0,27	0,65	0,13	0,02
F=0,3	0,90	2,84	2,33	0,69	0,24	0,65	0,15	0,02
F=0,4	0,69	2,23	1,94	0,61	0,22	0,64	0,17	0,02
F=0,5	0,56	1,83	1,66	0,55	0,21	0,63	0,20	0,03
F=1	0,29	0,97	0,96	0,37	0,15	0,59	2,15	0,61
Spinel lherzolite								
F	**La**	**Ce**	**Nd**	**Sm**	**Eu**	**Gd**	**Yb**	**Lu**
F=0,005	9,78	24,07	11,26	2,32	0,88	2,59	1,62	0,25
F=0,1	2,40	7,44	5,68	1,60	0,62	1,97	1,33	0,20

F=0,2	1,34	4,31	3,73	1,20	0,47	1,57	1,12	0,17
F=0,3	0,93	3,03	2,78	0,96	0,38	1,30	0,97	0,15
F=0,4	0,71	2,34	2,21	0,80	0,32	1,12	0,85	0,13
F=0,5	0,57	1,90	1,84	0,69	0,28	0,98	0,76	0,11
F=1	0,29	0,99	1,00	0,40	0,16	0,60	0,49	0,07

Note: The calculation was performed for the batch melting of the N-MORB source (MORBMA) **[10]** represented by garnet lherzolite, eclogite, and spinel lherzolite. The equations derived by Shaw **[25]** were used for the calculation.

Fig. 9. Chondrite-normalized REE distribution patterns in melt at various degrees of partial melting (F): (a) garnet lherzolite, (b) quartz eclogite, and (c) spinel lherzolite in comparison with the REE distribution in the model primary melt of the Central pluton.The initial REE contents in all models correspond to the level of the N-MORB source (MORBMA) **[10]**.

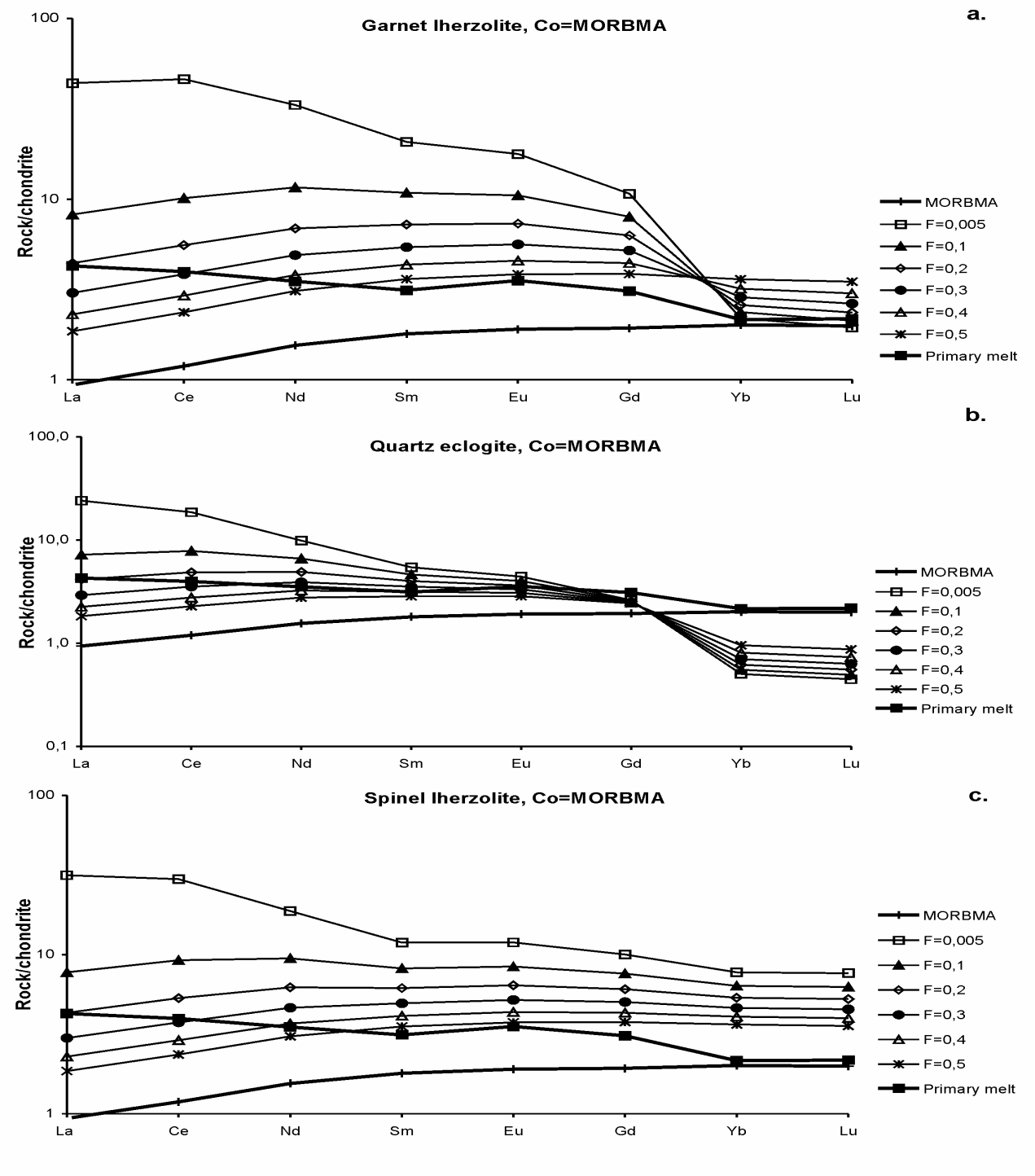

Fig. 10. MgO versus FeO as a criterion of primary composition for magmas formed by batch melting of mantle sources at a pressure of 30 kbar.
(1) Garnet lherzolite with Fo-92.06; (2) field of melts formed by melting of the hypothetical mantle source of the Central pluton (Fo-92.06); (3) bulk composition of the Vourinos ophiolite complex, Greece **[11]**; (4) field of melts formed by melting of a mantle source corresponding to

the composition of the Vourinos ophiolite complex; (5) melt derived from the hypothetical mantle source of the Central pluton (Fo-92.06) at a degree of melting of 28% (F = 0.28); (6) primary melt of the Central pluton; (7) marginal facies of the Central pluton **[2]**; and (8) primitive mantle with Fo-89.42 **[9]**.

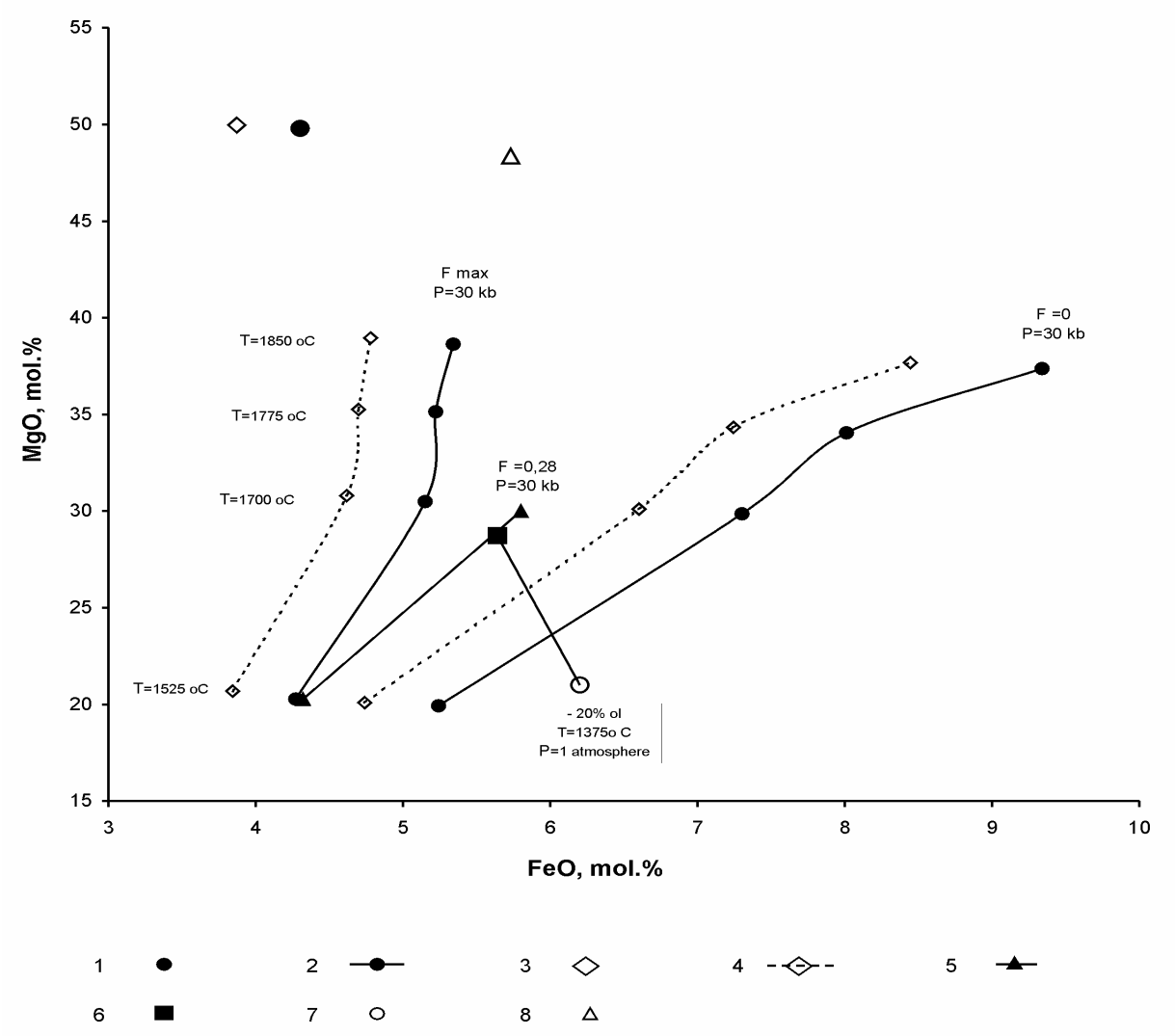

CONCLUSIONS

1. The Central pluton in the Lake Zone, western Mongolia belongs to the Cambrian peridotite-pyroxenite-anorthosite-gabbronorite association. It is a single-phase layered basic intrusion with a weighted mean picritic composition. The chilled, marginal facies, and layered series are recognized; the latter comprises the ultramafic, subultramafic, mafic, and anorthositic rock groups. The change of cumulus mineral assemblages in the section indicates the following

crystallization sequence: [Ol($Fo_{64.3}$) + Sp] - [Ol($Fo_{68.7-65.6}$) + Pl($An_{77.7}$) +/- Cpx (Mg# = 86.8-80.0)] - [+/- Ol($Fo_{66.5-54.5}$) + Pl($An_{89.3-68.6}$) + Cpx (Mg# = 87.5-78.5) + Opx (Mg# = 84.7-64.4)].

2. The primary magma that entered the intrusive chamber already contained about 20% of olivine crystals, which formed a basal peridotite unit at the chamber bottom. According to computer modeling by the COMAGMAT 3.5 program **[6]**, the whole magmatic series of the Central pluton including the basal peridotite unit could be formed by the sequential fractionation of major cumulus phases (olivine, plagioclase, and clinopyroxene). The modeling was performed in the regime of layered intrusion formation at 1 kbar, QFM buffer, and 0-0.5 wt % H_2O in the melt.

3. The geochemical signature of the Central pluton is typical of subduction-related magmas, particularly, of island-arc tholeiitic series. Trace element contents in the plutonic rocks, except for highly mobile U and Th, are comparable with those in the primitive mantle.

4. The primary melt of the Central pluton was formed in the environment of a primitive island arc from a mantle source similar in composition to the N-MORB source enriched in mobile component in the course of subduction.

5. The major and trace element composition of the primary melt and modeling by the MELTS program **[12]** indicate that it could be formed by partial melting of the depleted garnet lherzolite at a pressure of 25 kbar, a temperature of 1600°C, 0.1 wt % H_2O in the source, and 20% melting.

6. The Central pluton is probably a shallow-seated analogue of the coeval high-alumina volcanics of the Lake Zone. The parental melt of the volcanics was probably contaminated by crustal material and experienced magma mixing. The similar geochemical characteristics of the volcanic and plutonic rocks suggest the existence of a common garnet-bearing mantle source related to the subduction zone.

ACKNOWLEDGMENTS

I thank A.E. Izokh for his assistance and support of this work and V.M. Kalugin and V.N. Sharapov for helpful criticism. This work was supported by the Russian Foundation for Basic Research, project nos. 98-05-65266 and 01-05-65295.

REFERENCES

1. Izokh, A.E., Polyakov, G.V., Gibsher, A.S., et al., High-Alumina Layered Gabbroids in the Central Asian Fold Belt: Geochemistry, Age, and Geodynamics, Geol. Geofiz., 1998, vol. 39, no. 11, pp. 1565-1577.

2. Izokh, A.E., Polyakov, G.V., Krivenko, A.P., et al., Gabbroidnye formatsii Zapadnoi Mongolii (Gabbroid Associations of Western Mongolia), Novosibirsk: Nauka, 1990.

3. Ivanov, V.M. and Volokhov, I.M., The Shaman Gabbro-Pyroxenite-Dunite Layered Pluton of the Lysaya Gora Complex in the Western Sayan, in Rudnye formatsii i genezis endogennykh mestorozhdenii Altae-Sayanskoi oblasti (Types and Genesis of Endogenic Ore Deposits in the Altai-Sayan Region), Novosibirsk: Nauka, 1968, pp. 52-84.

4. Izokh, A.E., Polyakov, G.V., Krivenko, A.P., and Bognibov, V.I., Origin of Ultrabasic Rocks in Mongolian Layered Gabbroid Intrusions, in Petrologiya giperbazitov i bazitov

(Petrology of Ultrabasic and Basic Rocks), Polyakov, G.V., Ed., Novosibirsk: Nauka, 1990, pp. 84-99.

5. Bognibov, V.I., Polyakov, G.V., Kovalevskii, V.E., and Petrova, T.E., Compositions of Minerals and the Origin of Ultrabasic and Basic Rocks in the Brungan Peridotite-Pyroxenite-Gabbronorite Pluton, Eastern Tuva, in Petrologiya i rudonosnost' magmaticheskikh formatsii Sibiri (Petrology and Ore-Bearing Potential of Siberian Igneous-Rock Series), Novosibirsk: Nauka, 1983, pp. 93-126.

6. Ariskin, A.A., Frenkel, M.Ya., Barmina, G.S., and Nielsen, R.L., COMAGMAT: A Fortran Program to Model Magma Differentiation Process, Comp. Geosci., 1993, vol. 19, pp. 1155-1170.

7. Ariskin, A.A., Barmina, G.S., Ozerov, A.Yu., and Nielsen, R.L., Origin of the High-Alumina Basalts of Klyuchevskoi Volcano, Petrologiya, 1995, vol. 3, no. 5, pp. 496-521.

8. Boynton, W.V., Cosmochemistry of the Rare Earth Elements. Meteorite Studies, in Rare Earth Element Geochemistry, Amsterdam, 1984, pp. 63-114.

9. Sun, S.-S. and McDonough, W.F., Chemical and Isotopic Systematics of Oceanic Basalts: Implications for Mantle Composition and Processes, in Magmatism in the Ocean Basins, Saunders, A.D. and Norry, M.J., Eds., Geol. Soc. London Spec. Publ., 1989, vol. 42, pp. 313-345.

10. Hofmann, A.W., Chemical Differentiation of the Earth: The Relationship between Mantle, Continental Crust, and Oceanic Crust, Earth Planet. Sci. Lett., 1988, vol. 90, pp. 297-314.

11. Moores, E.M., Petrology and Structure of the Vourinos Ophiolitic Complex of Northern Greece, Geol. Soc. Am. Spec. Publ., 1970, vol. 118, pp. 1-74.

12. Ghiorso, M.S. Hirschmann, M.M., and Sack, R.O., MELTS: Software for Thermodynamic Modeling of Magmatic Systems, EOS, 1994, vol. 75, pp. 571-576.

13. Roeder, P.L. and Emslie, R.F., Olivine-Liquid Equilibrium, Contrib. Mineral. Petrol., 1970, vol. 29, pp. 275-89.

14. Jones, J.H., Temperature- and Pressure-Independent Correlations of Olivine/Liquid Partition Coefficients and Their Application to Trace Element Partitioning, Contrib. Mineral. Petrol., 1984, vol. 88, pp. 126-132.

15. Kadik, A.A., Lukanin, O.A., and Lapin, I.V., Fiziko-khimicheskie usloviya evolyutsii bazal'tovykh magm v pripoverkhnostnykh ochagakh (Physicochemical Conditions of Basaltic Magma Evolution in Shallow Chambers), Moscow: Nauka, 1990.

16. Kovalenko, V.I., Yarmolyuk, V.V., Pukhtel', I.S., et al., Igneous Rocks and Magma Sources of Ophiolites in the Ozernaya Zone, Mongolia, Petrologiya, 1996, vol. 4, no. 5, pp. 453-495.

17. Le Bas, M.J., Le Maitre, R.W., Streckeisen, A., and Zanettin, B., A Chemical Classification of Volcanic Rocks Based on the Total Alkali-Silica Diagram, J. Petrol., 1986, vol. 27, pp. 745-750.

18. Petrograficheskii Kodeks (The Petrographic Code), St. Petersburg, 1995.

19. Bogatikov, O.A. and Tsvetkov, A.A., Magmaticheskaya evolyutsiya ostrovnykh dug (Magmatic Evolution of Island Arcs), Moscow: Nauka, 1988.

20. Wager, L. and Brown, G., Layered Igneous Rocks, Edinburg: Oliver, 1968. Translated under the title Rassloennye izverzhennye porody, Moscow: Mir, 1970.

21. Cox, K.G., Bell, J.D., and Punqherst, R.J., Interpretatsiya izverzhennykh gornykh porod (Interpretation of Igneous Rocks), Moscow: Nedra, 1982.

22. Dostal, J. and Dupuy, C., Coulon.C. Rare-Earth Elements in High-Alumina Basaltic Rocks from Sardinia, Chem. Geol., 1976, vol. 18, pp. 251-262.

23. Morra, V., Secchi, F.A.G., Melluso, L., and Franciosi, L., High-Mg Subduction-Related Tertiary Basalts in Sardinia, Italy, Lithos, 1997, vol. 40, pp. 69-91.

24. Kerrich, R. and Wyman, D.A., Review of Developments in Trace-Element Fingerprinting of Geodynamic Settings and Their Implications for Mineral Exploration, Austral. J. Earth Sci., 1977, vol. 44, pp. 465-487.

25. Shaw, D.M., Trace Element Fractionation during Anatexis, Geochim. Cosmochim. Acta, 1970, vol. 34, pp. 237-243.

26. Fujimaki, H., Tatsumoto, M., and Aoki, K., Partition Coefficients of Hf, Zr, and REE between Phenocrysts and Groundmasses, J. Geophys. Res., 1984, vol. 89, Suppl.: Proc. Fourteenth Lunar Planet. Sci. Conf., part 2, pp. B662-B672.

27. Rollinson, H., Using Geochemical Data: Evaluation, Presentation, and Interpretation, Harlow: Longman, 1993.

28. Arth, J.G., Behavior of Trace Elements during Magmatic Processes: A Summary of Theoretical Models and Their Applications, J. Res. U.S. Geol. Surv., 1976, vol. 4, pp. 41-47.

29. Irving, A.J. and Frey, F.A., Distribution of Trace Elements between Garnet Megacrysts and Host Volcanic Liquids of Kimberlitic to Rhyolitic Composition, Geochim. Cosmochim. Acta, 1978, vol. 42, pp. 771-787.

30. Miller, D.M., Langmuir, C.H., Goldstein, S.L., and Franks, A.L., The Importance of Parental Magma Composition to Calc-Alkaline and Tholeiitic Evolution: Evidence from Umnak Island in the Aleutians, J. Geophys. Res., 1992, vol. 97, pp. 321-343.

31. Hanson, G.N. and Langmuir, C.H., Modeling of Major Elements in Mantle-Melt Systems Using Trace Element Approaches, Geochim. Cosmochim. Acta, 1978, vol. 42, pp. 725-741.

32. Ringwood, A.E., Composition and Petrology of the Earth's Mantle, New York: McGraw-Hill, 1975. Translated under the title Sostav i petrologiya mantii Zemli, Moscow: Nedra, 1981.

33. Herzberg, C. and Zhang, J., Melting Experiments on Anhydrous Peridotite KLB-1: Compositions of Magmas in the Upper Mantle and Transition Zone, J. Geophys. Res., 1996, vol. 101, no. B4, pp. 8271-8295.

34. Longhi, J., Liquidus Equilibria of Some Primary Lunar and Terrestrial Melt in the Garnet Stability Field, Geochim. Cosmochim. Acta, 1995, vol. 59, pp. 2375-2386.

35. Bickle, M.J., Ford, C.E., and Nisbet, E.G., The Petrogenesis of Peridotitic Komatiites: Evidence from High-Pressure Melting Experiments, Earth Planet. Sci. Lett., 1977, vol. 37, pp. 97-106.

36. Hirose, K. and Kushiro, I., Partial Melting of Dry Peridotites at High Pressures: Determination of Compositions of Melts Segregated from Peridotite Using Aggregates of Diamond, Earth Planet. Sci. Lett., 1993, vol. 114, pp. 477-489.

37. Hirschmann, M.M., Ghiorso, M.S., Wasylenki, L.E., et al., Calculation of Peridotite Partial Melting from Thermodynamic Models of Minerals and Melts. I. Review of Methods and Comparison with Experiments, J. Petrol., 1998, vol. 39, no. 6, pp. 1091-1115.